JOURNAL OF QUATERNARY SCIENCE (2020) 1–28 ISSN 0267-8179. DOI: 10.1002/jqs.3229

JQS Journal of Quaternary Science QRA Quaternary Research Association

The evolution of the terrestrial-terminating Irish Sea glacier during the last glaciation

RICHARD CHRISTOPHER CHIVERRELL,[1]* GEOFF STEPHEN POWELL THOMAS,[1] MATTHEW BURKE,[1] ALICIA MEDIALDEA,[2] RACHEL SMEDLEY,[1] MARK BATEMAN,[3] CHRIS CLARK,[3] GEOFFREY A. T. DULLER,[4] DEREK FABEL,[5] GERAINT JENKINS,[4] XIANJIAO OU,[4] HELEN MARIE ROBERTS[4] and JAMES SCOURSE[6]

[1]Geography and Planning, University of Liverpool, Liverpool, Merseyside, UK
[2]University of Cologne, Institute of Geography, Köln, Nordrhein-Westfalen, Germany
[3]Department of Geography, University of Sheffield, Sheffield, UK
[4]Department of Geography and Earth Sciences, Aberystwyth University, Aberystwyth, Ceredigion, UK
[5]Scottish Universities Environmental Research Centre, SUERC AMS Laboratory, East Kilbride, South Lanarkshire, UK
[6]Centre for Geography and Environmental Science, University of Exeter, Penryn, Cornwall, UK

Received 9 July 2019; Revised 21 April 2020; Accepted 13 June 2020

ABSTRACT: Here we reconstruct the last advance to maximum limits and retreat of the Irish Sea Glacier (ISG), the only land-terminating ice lobe of the western British Irish Ice Sheet. A series of reverse bedrock slopes rendered proglacial lakes endemic, forming time-transgressive moraine- and bedrock-dammed basins that evolved with ice marginal retreat. Combining, for the first time on glacial sediments, optically stimulated luminescence (OSL) bleaching profiles for cobbles with single grain and small aliquot OSL measurements on sands, has produced a coherent chronology from these heterogeneously bleached samples. This chronology constrains what is globally an early build-up of ice during late Marine Isotope Stage 3 and Greenland Stadial (GS) 5, with ice margins reaching south Lancashire by 30 ± 1.2 ka, followed by a 120-km advance at 28.3 ± 1.4 ka reaching its 26.5 ± 1.1 ka maximum extent during GS-3. Early retreat during GS-3 reflects piracy of ice sources shared with the Irish-Sea Ice Stream (ISIS), starving the ISG. With ISG retreat, an opportunistic readvance of Welsh ice during GS-2 rode over the ISG moraines occupying the space vacated, with ice margins oscillating within a substantial glacial over-deepening. Our geomorphological chronosequence shows a glacial system forced by climate but mediated by piracy of ice sources shared with the ISIS, changing flow regimes and fronting environments.

KEYWORDS: British–Irish ice sheet; deglaciation; geomorphology; glacial lakes; luminescence dating

Introduction

The eastern sector of ice masses located in the Irish Sea Basin (ISB) is unusual in the former British–Irish Ice Sheet (BIIS) in that it comprises an ice mass generated on land, passing offshore, and then flowing back onto land to maximum limits in the English Midlands (Fig. 1) (Thomas, 1989, 2005; Chiverrell and Thomas, 2010). This Irish Sea Glacier (ISG) is the only land-based terminus of the western outlets of the former BIIS, and unambiguous evidence (*sensu* Stokes and Clark, 1999; Stokes, 2018) for ice streaming is lacking. Repeated and complex ice-marginal oscillations during deglaciation characterize the retreat dynamics of the adjacent and linked marine-terminating western extension of this ice mass called the Irish Sea Ice Stream (McCabe *et al.*, 1998; Thomas *et al.*, 2004; Thomas and Chiverrell, 2007; McCabe, 2008; Livingstone *et al.*, 2010, 2012; Smedley *et al.*, 2017a, 2017b; Chiverrell *et al.*, 2018). The timing in which many glaciers and ice sheets reached their maximum extent in the last glacial cycle was out of phase, but broadly form a time window 27.5–19 ka termed the 'Last Glacial Maximum' (LGM) (Clark *et al.*, 2009; Hughes *et al.*, 2013; Hughes and Gibbard, 2015; Palacios *et al.*, 2020) that coincides with the time of minimum sea levels (Lambeck and Purcell, 2001; Lambeck *et al.*, 2014).

At the LGM in north-west England, the ISG flowed into the Cheshire–Shropshire lowlands and 125 km south to maximum limits in the English Midlands (Thomas, 2005; Worsley, 2005). The sediment landform assemblages in Cheshire–Shropshire have received less attention (Johnson, 1971; Morgan, 1973; Thomas, 1985b, 1989, 2005; Worsley, 2005; Parkes *et al.*, 2009) than other sectors of the ice sheet. Further north, recent comprehensive mapping (Chiverrell *et al.*, 2016) in lowland Lancashire shows that the landform signature reflects the uncoupling and realignment of adjacent and increasingly separate ice lobes that developed during deglaciation between 21 and 17.3 ka, showing the interaction of a dominant ISG with smaller ice masses draining eastern Cumbria and the Pennines. The geochronological data published to date suggest that rates of ice-marginal retreat in the eastern ISB were slower than the Irish Sea Ice Stream (ISIS) to the west (Chiverrell *et al.*, 2013, 2016, 2018; Smedley *et al.*, 2017a; Small *et al.*, 2018; Scourse *et al.*, 2019). These differences in the pace of retreat have been attributed to the absence of ice streaming and the terrestrial nature of the eastern terminating ice lobe (Chiverrell *et al.*, 2016).

Here we:

1. Reconstruct the patterns of ice-marginal retreat using new comprehensive ice-marginal landform and sediment–landform

*Correspondence: Richard Christopher Chiverrell, as above.
E-mail: rchiv@liv.ac.uk

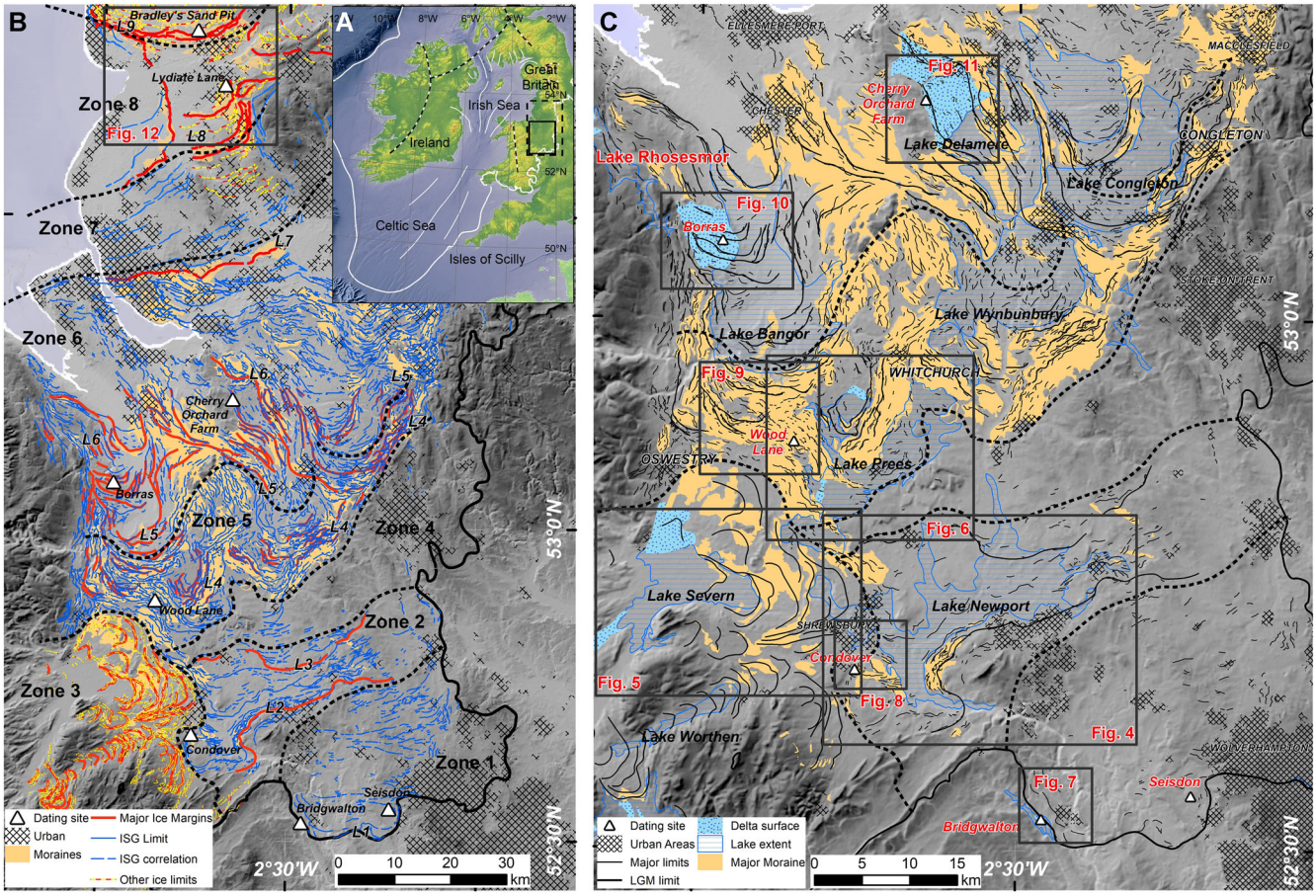

Figure 1. (A) Location and context of former ice masses in the Irish Sea sector plotted over the CGIAR-CSI SRTM (Version 4) 30-m-resolution (srtm.csi.cgiar.org/srtmdata/) and EMODnet topographic data (http://www.emodnethydrographyeu/). The extent of Fig. 1B (dashed) and Fig. 1C (solid) are shown. (B) Summary geomorphology overlain on a hillshaded elevation model showing the major and minor interpreted ice limits (limits L1 to L9). The ice limits differentiate the Irish Sea Glacier (ISG) (blue) and confluent ice systems issuing from Wales and the eastern Lake District/Pennines (yellow). The mapped area has been divided into nine labelled zones for description. Locations sampled for geochronology are identified. (C) More detailed geomorphology showing the major moraine, delta and former proglacial lake basins between L1 and L7. Extent rectangles show the areas covered in later maps and the locations sampled for geochronology. [Color figure can be viewed at wileyonlinelibrary.com]

data, including a reassessment of the distribution and nature of extensive proglacial lakes.
2. Define the primary glacial depositional environments and interpret the time–space sequence of ice dynamics using the sediment–landform assemblages.
3. Constrain, using a new optically stimulated luminescence (OSL) chronology, both the timing and the pace of deglaciation from LGM extent for this non-marine terminating margin and discuss its significance.
4. Evaluate the controls over ice dynamics during >200 km of ice-marginal retreat and the interaction with ubiquitous proglacial palaeo-lakes during that retreat.

Geological setting and topographical context

Glaciers have repeatedly invaded the lowlands of north-west England during the Pleistocene and at the LGM they extended south into the English Midlands (Fig. 1B). The region has been divided into nine zones to describe the glacial sediment landform assemblages and interpret the pattern and timing of ice retreat (Fig. 1B). Permo-Triassic sandstones and mudstones floor these lowlands, and are flanked by uplands of lower Palaeozoic strata in the west and fault-bounded sandstones and shales (Carboniferous) in the east (Earp *et al.*, 1961; Longworth, 1985; Aitkenhead *et al.*, 1992). Four bedrock highs cross the region and played a significant role in influencing ice flows and the ice-marginal dynamics during glacial retreat. These bedrock obstructions were the NE–SW aligned Wenlock Edge bedrock high (max. elevation ~250 m; Zone 1), and a series of Permo-Triassic bedrock uplands including in Zone 4 an arcuate E–W aligned ridge (max. ~180 m), in Zone 5 the N–S aligned sandstone hills of mid-Cheshire (max. 227 m) and in south Lancashire (Zone 7) an SW–NE aligned bedrock high (max. 175 m). The most substantial thicknesses of glacial sediment occur in the Severn Basin upstream of the Ironbridge Gorge (zones 2–3), the substantial Oswestry–Whitchurch–Congleton moraine belt (Pocock and Wray, 1925; Poole, 1966; Thomas, 1989; Parkes *et al.*, 2009), the Dee, Weaver, Mersey and Manchester basins (Zone 6), and the lowlands flanking the Ribble Valley (Zone 8) that includes the E–W ridges of the 'Kirkham Moraine' (Zone 9) (Gresswell, 1967; Chiverrell *et al.*, 2016).

Materials and methods

Geomorphology

The glacial geomorphology of the Cheshire–Shropshire–Staffordshire lowlands (12 000 km^2) (Fig. 1C) was mapped (Supporting Information Data 1) using the NEXTMap Great Britain digital terrain model following approaches identical to Chiverrell *et al.* (2016). These new data significantly extend the 4300-km^2 glacial geomorphological database for Lancashire (NW England) presented by Chiverrell *et al.* (2016). British Geological Survey

(BGS) digital solid and drift mapping was used to delimit bedrock at the surface. Geomorphological mapping followed the following process steps: (i) identifying the primary breaks in slope together with symbols for largely non-genetic landform geometries such as flats, ridges, mounds and basins; and (ii) interpretation of these forms using sediment–landform associations to produce a layered geomorphological ARCGIS geodatabase. Ground-truthing of the mapping was carried out in selected areas by conventional field investigation. Interpretation of the geomorphology follows conventional typologies for glacial landforms (e.g. Evans, 2003), and was underpinned by both the landform morphology and associated sediments.

Stratigraphy and sediment landform assemblages

Exposures of the glacial stratigraphy are limited across the region with sand and gravel quarries providing the main means of accessing sedimentary data. Sediment sequences were described at Bridgwalton (Bridgnorth), Seisdon (Wolverhampton), Condover (Shrewsbury), Wood Lane (Ellesmere), Borras (Wrexham), Cherry Orchard (Delamere), Lydiate Lane (Chorley) and Bradley's (Preston) quarries (Fig. 1B). Exposures were logged using field sketches, vertical lithofacies logs and photo-montages following standard procedures (Evans and Benn, 2004; Thomas *et al.*, 2004). Other characteristics recorded included textural classifications, sorting and grain size, palaeocurrents or till fabric indicators, sedimentary structures, nature of contacts and the lithofacies. The exposures at each of these locations were sampled for materials for OSL dating. Borehole data from over 89 000 locations were assessed using the BGS geodatabase, and this was reduced to 56 000 sites by excluding confidential, shallow (<3 m) or uncertain location boreholes. In general, these borehole records were used to corroborate the sediment–landform interpretations from the geomorphological mapping. For boreholes distributed across important geomorphological features, the records were classified from the descriptions into gravel, sand and gravel, sand, silt/clay, laminated silt/clay, and diamictons, and used to construct stratigraphical cross-sections. Ground elevations of the sections were interrogated from the NEXTMap digital elevation model and cross-checked against the borehole reports (Thomas, 1985a, 1989; Chiverrell *et al.*, 2008, 2016). Uncertainties in the interpretation of cross-sections arise from the inherent vertical and lateral variability in glacigenic sequences, the limited continuity of lithological markers between boreholes and uncertain origin for breaks in the borehole records (e.g. tectonic or cut and fill). However, combining the regional geomorphology with the borehole cross-sections gives us some confidence in these interpretations.

Dating the retreat of the Irish Sea lobe

Geochronological strategy and field sampling

Samples for OSL dating were collected from eight sites targeting glacifluvial and deltaic outwash sands and gravels, which were selected based on their ice-proximal context and potential to date well-defined ice margins (Fig. 1B; Table 1). The principle underpinning OSL dating is that exposure to sunlight zeros or bleaches an OSL signal that develops within mineral grains (typically quartz or K-feldspar). During burial, the materials are exposed to natural radiation which increases the charge stored within the quartz or feldspar, resulting in a larger OSL signal as the period of burial increases. Here we use three approaches to OSL dating to constrain the burial age of glacial outwash sediments. The first two approaches used single grains (SG) and small aliquots (SA; ~20 grains) of sand-sized quartz grains separated from sediments (Murray and Wintle, 2000; Duller, 2008). The third and more experimental approach targets the feldspar grains within buried cobbles (Freiesleben *et al.*, 2015; Sohbati *et al.*, 2015; Jenkins *et al.*, 2018). The cobble-based approach uses the variation of the luminescence signal into the cobble sub-surface to assess whether it was completely bleached or not during its last exposure to daylight; this is a major advantage in a heterogeneously bleached environment. For OSL dating of sand-sized grains the measurement of multiple replicates (typically here ~50) can also identify those grains in a heterogeneously bleached sample that were exposed to sunlight most recently (typically referred to as being well bleached), where statistical models are required to determine an accurate age, e.g. the Minimum Age Model (MAM) (Galbraith *et al.*, 1999). All these luminescence methods date the last exposure of the minerals to daylight, and it is assumed that this relates to the last depositional cycle. For the sand samples from Seisdon, Bridgwalton, Condover, Wood Lane, Borras, Cherry Orchard, Lydiate Lane and Bradley's quarries (Fig. 1B), opaque tubes were hammered into sedimentary sections to prevent exposure to sunlight during sampling. At Bridgwalton Quarry and Lydiate Lane, granite cobbles were obtained from gravel-dominated lithofacies. Cobbles were sampled into light-tight bags under dark conditions using an opaque black sheet, targeting cobbles with *b*-axes varying from ~10 to 3 cm and recording the clast orientation by marking the upper and lower surfaces (Jenkins *et al.*, 2018). The sediment matrix around the cobbles was collected for dosimetry.

Optically stimulated luminescence dating

The sample preparation and analysis methods used were identical to existing studies for SG-OSL dating (Smedley *et al.*, 2017a, 2017b), SA-OSL dating (Evans *et al.*, 2017) and cobble dating (Jenkins *et al.*, 2018). For all samples, the external gamma dose rates were determined using *in situ* gamma spectrometry. For sand-sized samples, external beta dose rates were calculated from U, Th, K and Rb concentrations that were determined using inductively coupled plasma mass spectrometry (ICP-MS) and inductively coupled plasma atomic emission spectroscopy (ICP-AES). For the cobbles, thick source beta counting using a Risø GM-25-5 instrument (Bøtter-Jensen and Mejdahl, 1988) was used to determine the external beta dose. The dose rate to individual rock slices originates additionally from radionuclides within the cobble. To measure this, a sample of each cobble and a sample of the surrounding matrix were milled to a fine powder for dosimetry measurements (Jenkins *et al.*, 2018). The dose rate to feldspar grains in the cobble also included an internal beta dose contribution arising from the K-content of the grains (assumed to be $12.5 \pm 0.5\%$ as per Huntley and Baril, 1997). Appropriate conversion factors (Guérin *et al.*, 2011, 2012) were applied to calculate the final total dose rate (Table 1) including grain size. In terms of palaeomoisture attenuation, all the sampled sites have water tables that are presently artificially low, owing to sand and gravel extraction and all have water management strategies (e.g. settling lagoons) indicative of higher natural water tables. Maximum pore spaces in 180–250-μm sand are in the range between rhombohedral (26%) and random (40%) packing, which for moderately sorted rounded to sub-rounded sands equates to saturated water contents of around 30%. The inter-annual pattern in the water table levels probably shows a summer draw-down of 2–3 m and water tables varying within 8–4 m of the ground surface for three sites in NW England with Permo-Triassic sandstone bedrock overlain by glacial sediments. This is probably representative of post-glacial water tables at these sites (BGS: http://www.bgs.ac.uk/research/groundwater/datainfo/NWRA.html). On this basis, for sediment samples moisture contents of $23 \pm 5\%$ were used for shallow and drier samples and $27 \pm 5\%$ for deeper saturated samples. In this study, for rock slices more than 1.5 mm below cobble

Table 1. Radioactivity and dose rate data for luminescence samples.

Site	Sample	Depth (m)	Water (%)	U (p.p.m.)*	Th (p.p.m.)*	K (%)*	Rb (p.p.m.)*	Beta dose rate (Gy ka^{-1})	Gamma dose rate (Gy ka^{-1})	Cosmic dose rate (Gy ka^{-1})	Total dose rate (Gy ka^{-1})
Seisdon	T3SEIS01	20	23	1.10	3.8	1.6	56.0	1.02 ± 0.12	0.56 ± 0.04	0.06 ± 0.01	1.66 ± 0.12
	T3SEIS02	20	23	1.08	3.3	1.8	55.1	1.15 ± 0.10	0.43 ± 0.03	0.03 ± 0.00	1.64 ± 0.10
Bridgwalton	T3BRID02	6	23	0.70	2.7	1.1	43.6	0.70 ± 0.06	0.46 ± 0.03	0.10 ± 0.01	1.24 ± 0.07
	T3BRID03	40	23	0.70	2.7	1.1	43.4	0.70 ± 0.06	0.42 ± 0.03	0.07 ± 0.00	1.20 ± 0.07
	T3BRID04	3	23	0.89	3.7	1.1	46.9	0.73 ± 0.06	0.50 ± 0.03	0.14 ± 0.01	1.39 ± 0.07
	T3BRID05	3.5	23	0.73	2.7	1.0	41.3	0.65 ± 0.06	0.40 ± 0.03	0.13 ± 0.01	1.19 ± 0.06
	T3BRID06†	5	n/a	2.23	6.8	3.9	–	4.58 ± 0.88	0.70 ± 0.03	0.12 ± 0.06	5.44 ± 0.88†
	T3BRID07	3	27	0.94	3.6	1.0	42.2	0.68 ± 0.04	0.58 ± 0.04	0.11 ± 0.01	1.38 ± 0.06
Condover	T3COND02	6.5	23	0.90	3.9	1.0	43.1	0.68 ± 0.06	0.40 ± 0.03	0.09 ± 0.01	1.20 ± 0.06
	T3COND04	1.5	23	0.70	2.7	1.0	42.8	0.64 ± 0.06	0.37 ± 0.02	0.17 ± 0.01	1.21 ± 0.06
	T3COND05	2.8	23	0.66	2.3	1.0	38.8	0.63 ± 0.06	0.05 ± 0.02	0.15 ± 0.01	1.14 ± 0.06
Wood Lane	T3WOOD04	14	23	0.92	3.0	1.2	46.7	0.77 ± 0.07	0.42 ± 0.02	0.05 ± 0.00	1.26 ± 0.07
	T3WOOD05	15	23	0.80	2.7	1.2	46.9	0.76 ± 0.07	0.47 ± 0.03	0.03 ± 0.00	1.29 ± 0.07
Cherry Orchard Farm	T3COF03	4	23	0.71	2.6	1.0	39.8	0.68 ± 0.07	0.40 ± 0.03	0.12 ± 0.01	1.22 ± 0.07
	T3COF04	3	23	0.60	2.1	1.0	37.9	0.67 ± 0.07	0.31 ± 0.02	0.14 ± 0.01	1.13 ± 0.07
Borras	T3BORR01	11	27	1.15	3.4	1.0	43.2	0.65 ± 0.05	0.38 ± 0.03	0.06 ± 0.00	1.11 ± 0.06
	T3BORR02	5	27	0.93	3.0	1.3	39.3	0.73 ± 0.06	0.39 ± 0.03	0.11 ± 0.01	1.25 ± 0.07
	T3BORR03	2	23	1.15	4.2	1.2	52.2	0.88 ± 0.07	0.48 ± 0.03	0.16 ± 0.01	1.54 ± 0.08
Dingle	T3DING01	1.5	15	0.59	1.7	0.9	35.5	0.63 ± 0.06	0.44 ± 0.02	0.17 ± 0.01	1.26 ± 0.06
	T3DING02	1.5	15	0.66	2.5	1.3	51.3	0.90 ± 0.08	0.41 ± 0.02	0.17 ± 0.01	1.49 ± 0.08
Lydiate Lane	T3LYDL04	5	23	0.68	2.4	1.4	50.7	0.85 ± 0.08	0.43 ± 0.03	0.11 ± 0.01	1.41 ± 0.08
	T3LYDL05	5.3	23	0.68	2.5	1.5	58.5	0.91 ± 0.09	0.42 ± 0.03	0.11 ± 0.01	1.45 ± 0.09
	T3LYDL06	4.0	23	1.22	2.5	0.9	–	0.66 ± 0.03	0.38 ± 0.03	0.12 ± 0.01	1.18 ± 0.04
	T3LL1D-04†	2.5	n/a	3.92	7.2	4.5	–	4.75 ± 1.01	0.84 ± 0.03	0.15 ± 0.04	5.80 ± 1.02
	T3LL1D-09†	2.5	n/a	3.39	6.7	4.5	–	5.47 ± 0.73	0.76 ± 0.04	0.15 ± 0.04	6.43 ± 0.74
Bradleys	T3BRAD03	5	23	0.72	2.5	1.6	58.2	0.96 ± 0.09	0.48 ± 0.03	0.11 ± 0.01	1.56 ± 0.09
	T3BRAD04	5	23	0.70	2.5	1.6	60.1	0.97 ± 0.09	0.47 ± 0.03	0.11 ± 0.01	1.56 ± 0.09
	T3BRAD06	4.5	23	1.23	1.9	1.1	–	0.76 ± 0.04	0.40 ± 0.02	0.12 ± 0.01	1.29 ± 0.05

*The analytical chemistry laboratory did not provide uncertainties on individual U, Th, K or Rb concentrations. Based on replicate analyses, uncertainties of 10% were assumed for U, Th and Rb, and 5% for K, and these uncertainties were propagated through the dose rate calculations.

†T3BRID06, LL1D-4 and -09 were cobbles. Geochemical data shown here are for the cobbles themselves, which dominates the dose rate beyond a depth of ~1.5 mm into the cobble. The dose rate varies slightly with depth. The dose rate values given here are the doses delivered to grains of K-feldspar averaged over the section of the cobbles thought to have been bleached at deposition. The depth to which cobbles were bleached is given in Table 2.

surfaces, ~90% of the dose rate comes from the cobble itself and not from the surrounding sediment matrix, making the dose rate effectively independent of the water content of the surrounding sediment; this is one of the benefits of deriving OSL ages from cobbles.

OSL analyses of all sand quartz samples were performed on grain sizes within the range of 180–250 μm (Table 2), with SA-OSL using aliquots each containing ~20 grains. Given that the proportion of quartz grains emitting an OSL signal for the samples in this study was small, it was thought likely that the SA-OSL signal was dominated by few grains. This has been shown to be the case elsewhere (e.g. Evans *et al.*, 2017). The equivalent dose (D_e) distributions determined using SG-OSL and SA-OSL are shown in Fig. 2. All SG-OSL and SA-OSL D_e distributions were asymmetrically distributed with high over-dispersion (OD; Table 2). As a result, it would appear likely that all samples had been heterogeneously bleached before burial. MAMs were therefore used to identify the well-bleached component of the heterogeneously bleached D_e distribution to determine the D_e values used for age calculation (Table 2). For SG-OSL the MAM of Galbraith and Laslett (1993) was used with σ_b determined for each sample by combining in quadrature the intrinsic OD determined from dose recovery experiments with the extrinsic scatter arising from external microdosimetry (~20%) (see Smedley *et al.*, 2017b, 2020). Due to averaging effects of potentially measuring 2–3 bright grains per aliquot using SA-OSL, it was more difficult to characterize the well-bleached component of the heterogeneously bleached D_e distribution. Final D_e values for age calculation using the SA-OSL were calculated using the internal–external uncertainty (IEU) model (Thomsen *et al.*, 2007) with the parameters *a* and *b* used in the model determined from dose recovery tests (calculating the OD of the dose distribution at multiple given doses) for each site. Such an approach has been applied successfully to glacial sediments elsewhere in the BIIS (e.g. Bateman *et al.*, 2018). Inter-comparison of SG-OSL with SA-OSL methods (Fig. 2) when applied to the same samples show similar ages for samples T3COND4 (SG-OSL 35.1 ± 6.8 ka, SA-OSL 34.3 ± 4.3 ka), T3BORR01 (SG-OSL 23.7 ± 3.2 ka, SA-OSL 22.9 ± 2.3 ka) and T3COF04 (SG-OSL 27.6 ± 4.2 ka, SA-OSL 29.1 ± 4.3 ka). However, the results for the two methods diverge for T3SEIS02 (SG-OSL 48.8 ± 8.4 ka, SA-OSL 22.9 ± 3.4 ka) and T3WOOD05 (SG-OSL 29.2 ± 4.3 ka, SA-OSL 19.8 ± 2.6 ka), which is potentially due to a lack of data characterizing the D_e distribution using SG-OSL ($n = 44$ grains for T3WOOD05 and $n = 41$ grains for T3SEIS02).

When using cobbles for luminescence dating, rock cores (either 7 or 8 mm in diameter and between 10 and 20 mm deep) were obtained from the upper face of cobbles under subdued red light. The cores were then cut, producing rock slices of 0.7 mm (Bridgwalton) or 0.4 mm (Lydiate Lane) thickness using a water-cooled diamond-edged wafering blade. The clean and dry rock slices were placed into steel planchettes for IRSL measurements. To screen rapidly whether the cobbles had been exposed to light before deposition, a single surface slice was taken and the L_n/T_n ratio was measured, the ratio of the natural (L_n) and an applied test (T_n) dose (~34 Gy at Bridgwalton and ~42 Gy at Lydiate Lane), for both the $IRSL_{50}$ and the post-IR $IRSL_{225}$ signals using a single cycle of the measurement procedure (Jenkins *et al.*, 2018). At Bridgwalton, out of 21 cobbles sampled, only one granite cobble yielded evidence of bleaching at deposition and subsequent measurements focused on that cobble, while at Lydiate Lane two of the 12 cobbles measured appeared to have been bleached. For the cobble from Bridgwalton, dose recovery measurements were performed on rock slices (Jenkins *et al.*, 2018) using a SOL-2 solar simulator for 7 days to reset any remaining residual signal. The six rock slices used for dose recovery measurements (three used for residual dose measurements and three given a known dose of 85.6 Gy) were taken from the same cobble as those rock slices that were used to determine an age. Measurements show that the $IRSL_{50}$ signal gives a residual–subtracted dose recovery ratio of 0.90 ± 0.02 and the post-IR $IRSL_{225}$ signal a ratio of 0.97 ± 0.03, confirming the suitability of this measurement protocol. Anomalous fading can be a significant issue when dating using feldspars (e.g. Huntley and Lamothe, 2001). Measurements of fading were undertaken on four or five different rock slices for each cobble. Rock slices were irradiated (43 or 150 Gy, Table 3) and preheated before storage for periods up to 1 month to allow calculation of g-values (Auclair *et al.*, 2003). The average *g*-values obtained were typically 1.4% per decade for the $IRSL_{50}$ signal, and 0.7% per decade for the post-IR $IRSL_{225}$ signal. Given the similarity of the fading rate measured for the $IRSL_{50}$ signal and the apparent quartz OSL fading rates (1.3 ± 0.3% per decade) (Thiel *et al.*, 2011), no correction has been made here for fading of either the $IRSL_{50}$ or the post-IR $IRSL_{225}$ signals.

A single aliquot regenerative dose (SAR) protocol modified for use on rock slices (Jenkins *et al.*, 2018) was used to generate D_e values using both the $IRSL_{50}$ signal and the post-IR $IRSL_{225}$ signal. The changes in L_n/T_n and D_e with depth were measured (Fig. 3). For three cobbles (T3BRID06, T3LL1D-04 and T3LL1D-09) the data confirm that the outermost part was well-bleached, with low $IRSL_{50}$ and post-IR $IRSL_{225}$ L_n/T_n ratios and D_e values at the surface gradually increasing at depth. The D_e values from slices that had been reset at deposition were then divided by the dose rate to give the age (Fig. 3; Table 2). For T3BRID06 the average age of the upper seven rock slices for the $IRSL_{50}$ signal is 25.3 ± 1.6 ka. The post-IR IRSL ages (29.3 ± 2.4 ka, Fig. 3a) are consistently greater than the $IRSL_{50}$ ages and this has also been observed in other cobble-dating studies (Freiesleben *et al.*, 2015; Jenkins *et al.*, 2018). It is unclear, at present, why there is a difference between the two signals, but the $IRSL_{50}$ ages are used here given that they are thought to be more reliable based on the agreement of $IRSL_{50}$ ages from cobbles and independent age control at Orrisdale Head, Isle of Man (Jenkins *et al.*, 2018). At Lydiate Lane (Fig. 3b,c) the post-IR $IRSL_{225}$ signal does not appear to have been bleached at the surface for either of the cobbles. The post-IR $IRSL_{225}$ signal is known to bleach much more slowly in daylight than the $IRSL_{50}$ signal (Colarossi *et al.*, 2015; Ou *et al.*, 2018). For two of the cobbles (T3LL1D-04 and T3LL1D-09) the $IRSL_{50}$ signal does appear to have been reset in the uppermost three slices and seven slices, giving ages of 30.2 ± 1.1 and 30.3 ± 1.4 ka, respectively (Fig. 3b,c).

Bayesian age modelling

The deglaciation sequence interpreted from the geomorphology provides here a prior model (i.e. the hypothetical 'relative-order' of events) for Bayesian modelling of the geochronological determinations (e.g. Chiverrell *et al.*, 2013). This Bayesian prior model was developed independently of the age information and included all geochronological samples (Bronk Ramsey, 2008, 2009a, 2009b; Bronk Ramsey and Lee, 2013; Buck *et al.*, 1996). The prior model here covers the ice-marginal retreat from maximum limits in the English Midlands through well-defined ice margin configurations in lowland Shropshire, Cheshire and Lancashire (Chiverrell *et al.*, 2016). The Bayesian modelling used a uniform phase sequence model punctuated by boundaries and was coded using OxCal 4.3 (Bronk Ramsey and Lee, 2013). The approach uses Markov chain Monte Carlo (MCMC) sampling to build up a distribution of possible solutions, generating a probability

Table 2. Luminescence equivalent dose and age data.

Site	Sample	Labcode	Analysis	Grain size (μm)	DR OD (%)	Total analysed*	*n**	OD (%)	Age model†	*a* value or Sigma*b*‡	D_e (Gy)	Age (ka)
Seisdon	T3SEIS01	Aber-SEIS01	SG	180–212	6	3600	61	86	MAM	0.20	97.4 ± 17.7	58.5 ± 11.5
	T3SEIS02	Shfd12096	SA	125–180	27	77	36	90	IEU	0.30	37.5 ± 5.0	22.9 ± 3.4
	T3SEIS02	Shfd12096	SG	125–180		4300	41	55	MAM	0.30	79.8 ± 12.8	48.8 ± 8.4
Bridgwalton	T3BRID02	Shfd16123	SA	212–250		80	47	54	IEU	0.25	63.8 ± 3.5	50.3 ± 3.9
	T3BRID03	Shfd16124	SA	212–250		80	43	49	IEU	0.25	36.0 ± 9.4	30.1 ± 8.0
	T3BRID04	Shfd14029	SA	212–250	23	121	51	59	IEU	0.25	35.0 ± 5.4	25.2 ± 4.1
	T3BRID05	Shfd14030	SA	212–250		58	40	92	IEU	0.25	34.5 ± 3.8	29.0 ± 3.5
	T3BRID06	Aber-BWT03-1	Cobble	360–820§		5.5*	7	n/a	WM	n/a	137 ± 7.8§	25.3 ± 1.6§
	T3BRID07	AberBRID07	SG	212–250	9	5700	54	79	MAM	0.20	38.2 ± 5.0	27.6 ± 3.8
Condover	T3COND02	Shfd16125	SA	212–250		98	67	68	IEU	0.15	23.6 ± 2.7	19.7 ± 2.5
	T3COND04	Shfd14031	SA	212–250	14	66	38	56	IEU	0.15	41.4 ± 4.7	34.3 ± 4.3
	T3COND04	Shfd14031	SG	212–250		6100	44	68	MAM	0.25	42.4 ± 7.9	35.1 ± 6.8
	T3COND05	Shfd14032	SA	212–250		48	24	67	IEU	0.15	65.9 ± 7.8	57.8 ± 7.8
Wood Lane	T3WOOD04	Shfd14033	SA	212–250		120	52	47	IEU	0.10	26.7 ± 3.3	21.2 ± 2.9
	T3WOOD05	Shfd14034	SA	212–250	8	150	64	66	IEU	0.10	25.5 ± 3.1	19.8 ± 2.6
	T3WOOD05	Shfd14034	SG	212–250		4700	44	70	MAM	0.20	37.7 ± 6.6	29.2 ± 5.4
CherryOrchard Farm	T3COF03	Aber-T3COF03	SG	180–212	6	5500	72	84	MAM	0.20	34.1 ± 4.7	27.9 ± 4.2
	T3COF04	Aber-T3COF04	SG	180–212	6	7100	67	69	MAM	0.20	31.1 ± 4.3	27.6 ± 4.2
	T3COF04	ShfdT3COF04	SA	180–212	25	104	64	76	IEU	0.20	32.8 ± 4.4	29.1 ± 4.3
Borras	T3BORR01	Shfd15029	SA	212–250		84	38	85	IEU	0.25	24.8 ± 2.2	22.9 ± 2.3
	T3BORR01	Aber-T3BORR01	SG	212–250	9	4600	69	62	MAM	0.20	26.3 ± 3.2	23.7 ± 3.2
	T3BORR02	Shfd14035	SA	212–250	24	82	37	62	IEU	0.25	36.4 ± 2.9	29.2 ± 2.8
	T3BORR03	Shfd14036	SA	212–250		54	26	64	IEU	0.25	35.4 ± 3.0	22.9 ± 2.3
Dingle Bank	T3DING01	Shfd14037	SA	212–250		102	39	36	FMM	0.20	15.9 ± 0.9	12.6 ± 1.0
	T3DING02	Shfd14038	SA	212–250		103	52	36	FMM	0.20	16.5 ± 0.7	11.1 ± 0.8
Lydiate Lane	T3LYDL04	Shfd14039	SA	212–250	26	107	56	83	IEU	0.25	42.8 ± 3.2	30.9 ± 5.2
	T3LYDL05	Shfd14040	SA	212–250		108	46	86	IEU	0.25	64.4 ± 4.2	44.5 ± 3.9
	T3LYDL06	Aber-T3LYDL06	SG	212–250	38	6000	47	65	MAM	0.45	67.2 ± 15.1	57.2 ± 13.1
	T3LL1D-04	Aber-LL1D-04	Cobble	260–820§		2.1*	6	n/a	WM	n/a	176 ± 13	30.2 ± 1.1
	T3LL1D-09	Aber-LL1D-09	Cobble	430–1150§		5.0*	7	n/a	WM	n/a	196 ± 11	30.3 ± 1.4
Bradleys	T3BRAD03	Shfd14041	SA	212–250	17	112	68	71	IEU	0.20	44.8 ± 2.8	28.7 ± 2.5
	T3BRAD04	Shfd14042	SA	212–250		93	51	86	IEU	0.20	39.3 ± 2.7	25.2 ± 2.3
	T3BRAD06	Aber-T3BRAD06	SG	212–250	19	7900	125	53	MAM	0.30	59.0 ± 6.4	45.7 ± 5.2

*Total analysed is the number of small aliquots or single grains measured for a sample, while the column headed '*n*' is the number of small aliquots of single grains accepted for D_e modelling. For T3BRID06, LL1D-04, and -09, which were cobbles, the 'Total analysed' is the depth to which the cobble is thought to be bleached in millimetres, and '*n*' is the number of rock slices measured in this part of the cobble.
†For single grain measurements the minimum age model (MAM) was used, while the internal–external uncertainty (IEU) model was used for single aliquot data. For the cobbles (T3BRID06, LL1D-04 and -09) the weighted mean of the bleached slices was used.
‡Where the IEU model was used, the first parameter '*a*' is given in this column. The second parameter '*b*' is 1.5 for all samples. For samples analysed using the MAM, the value given here is that for sigma *b*.
§T3BRID06, LL1D-04, and -09 were cobbles. The grain size is an estimate for the K-feldspar grains within the cobble. The D_e given here is for illustrative purposes only, and is the average value for the section of the cobble that is thought to have been bleached at deposition. Ages were calculated for each slice, and the age for each cobble was calculated as the average of the ages for the slices that were bleached at deposition (Fig. 3).

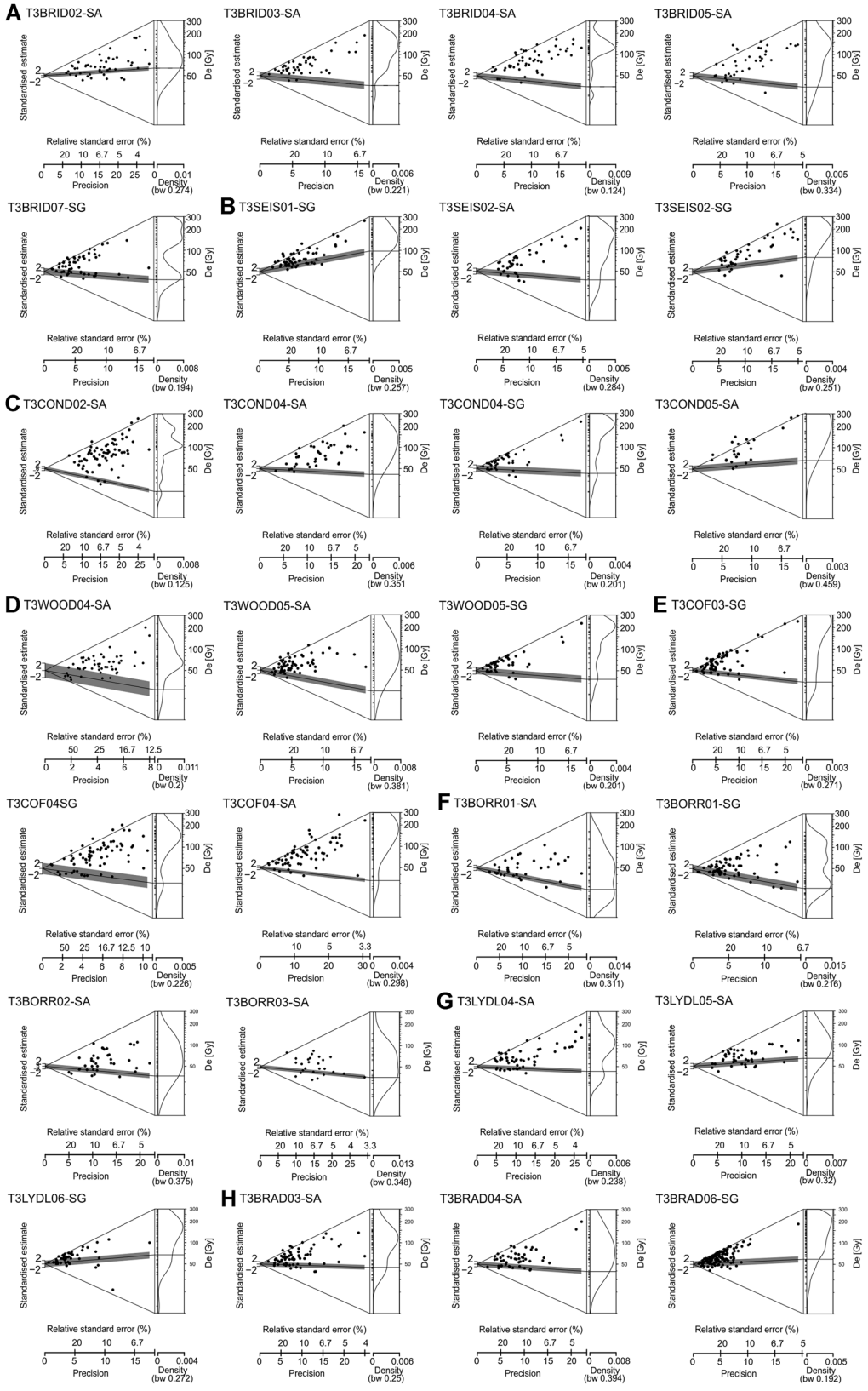

Figure 2. Optically stimulated luminescence data. Abanico plots (Dietze *et al.*, 2016) of the D_e values determined for OSL dating applied at (A) Bridgwalton, (B) Seisdon, (C) Condover, (D) Wood Lane, (E) Cherry Orchard Farm, (F) Borras, (G) Lydiate Lane and (H) Bradley's Quarries. The plots present the D_e distributions in two plots that share a common *z*-axis of D_e values: (i) a bivariate plot where each D_e value is presented in relation to its precision (shown on the *x*-axis, where those more precisely known are plotted to the right) – this is similar to the radial plot commonly used in luminescence dating; and (ii) a univariate plot showing the age frequency distribution of D_e values, which does not give any presentation of the precision of individual D_e values. The grey shading across both plots shows the D_e used in age calculation for each distribution (2σ shown on the *y*-axis). The combination of these two plots aids interpretation of the scatter in the D_e distributions, where samples with a greater range of D_e values on the *z*-axis have larger amounts of scatter in the D_e distribution.

Table 3. Fading measurements for the three cobbles. The number of slices measured for each cobble is given in the column headed '*n*'.

Site	Sample	Given dose (Gy)	*n*	$IRSL_{50}$ fading rate (%/decade)	Post-IR $IRSL_{225}$ fading rate (%/decade)
Bridgwalton	Aber-T3BRID06	43	5	1.41 ± 0.63	0.67 ± 0.62
Lydiate Lane	Aber-T3LL1D-04	150	4	1.48 ± 0.014	0.81 ± 0.26
	Aber-T3LL1D-09	150	4	1.39 ± 0.75	0.73 ± 0.30

called a posterior density estimate, which is the product of both the prior model and the likelihood (measured ages) probabilities for each sample. This approach generates modelled ages for boundaries for a series of ice margin limit positions between the major zones (L1 to L9: Fig. 1B). Each retreat Zone was coded as a Phase and contained grouped dating information for sites that shared a common relationship with the adjacent zones. Phases were delimited by the Boundary command and generated a modelled age probability distribution output for each ice limit (L1, L2, L4, L5, L6, L8 and L9).

The age model uses the new geochronological data alongside three other clusters of geochronological information. Predating the advance of ice in the region, organic sediments at Four Ashes (Staffordshire) have previously been ^{14}C dated to around 35–34 cal ka BP (Morgan, 1973) and Telfer *et al.* (2009) used OSL to date loessal deposits in north Lancashire to 27.2 ± 2.6 ka. In the Bayesian model, these ages pre-dating the ice advance are grouped as a Phase at the beginning of the Prior model. Later in the Prior model the ice margins pass north from the region to limits identified and dated in north Lancashire (Telfer *et al.*, 2009), on the Isle of Man and coastal Cumbria (Chiverrell *et al.*, 2018). Deglacial loessal deposits at Warton Crag (north Lancashire) have been OSL dated to 19.3 ± 2.6 ka (Telfer *et al.*, 2009), and ice-marginal outwash deposits at Turkeyland, SE Isle of Man, and Gutterby, SW Cumbria, have been SG-OSL dated to 19.2 ± 2 and 21.7 ± 2.6 ka, respectively (Chiverrell *et al.*, 2018). Together these three age estimates form a grouping immediately post-dating the passage northwards of ice margins from the Lancashire and Cheshire region. The ultimate decline of ice from the region is recorded by a series of cosmogenic isotope surface exposure ages from glacigenic features and materials, and these date a series of erratic boulders south of Shap in east Cumbria to 17.35 ± 0.5 ka (Wilson *et al.*, 2013), the erratic boulders at Norber in the Pennines to 17.9 ± 1.0 ka (Wilson *et al.*, 2012a; Wilson and Lord, 2014), and boulders from a series of moraines in the Duddon Valley, SW Cumbria, dated to 16.5 ± 0.8 ka (Wilson *et al.*, 2018). The Sequence model was run to assess outliers in time using a Student's *t*-distribution ($p < 0.05$) to describe the outlier distribution and a scaling of 10^0–10^4 years (Bronk Ramsey, 2009b). Obvious outliers were given a probability scaling of $p = 1$, with ages that fit poorly within the model allocated probabilities of $p < 0.25$, $p < 0.5$, $p < 0.75$ and $p < 0.95$ on a scale of increasing outlier severity.

Results

Sediments and landforms of the Shropshire–Lancashire lowlands

At the LGM, ice sourced dominantly in southern Scotland and Cumbria converged as a coherent ice mass in the eastern Irish Sea and expanded reaching maximum limits in the English Midlands (Fig. 1B) (Chiverrell and Thomas, 2010; Clark *et al.*, 2012). In the Lancashire–Cheshire–Shropshire lowlands this ISG interacted with glaciers issuing from the Welsh Borderlands to the west (Thomas, 2005) and Pennines to the east (Chiverrell *et al.*, 2016). Ice contact marginal and proglacial landforms dominate the geomorphological record of these lowlands (Supporting Information Data 1), with streamlined glacial bedforms lacking, which reflects either erosion, sediment burial or perhaps a lack of ice-streaming in this sector. The sediment landform assemblages are dominated by moraines, sandur flats and former lake basins (Fig. 1C; Supporting Information Data 1), and these reflect the oscillations and retreat dynamics of the ice margin. The geometry of former ice margins (Fig. 1B) reconstructed from the distribution of ice-marginal landforms shows the progressive unzipping of the ISG from tributary ice masses.

During the extension to LGM limits ice descended over the Wenlock Edge into the Severn, Worfe and Stour Valleys (Zone 1). The terrain is gently undulating and covered by thin and localized glacial sediments. Moraine ridges are scarce, which is interpreted as reflecting that ice-marginal retreat was relatively rapid. The few moraines form a broad arcuate lobe at the maximum extent (Fig. 1C), but are dissected by deeply

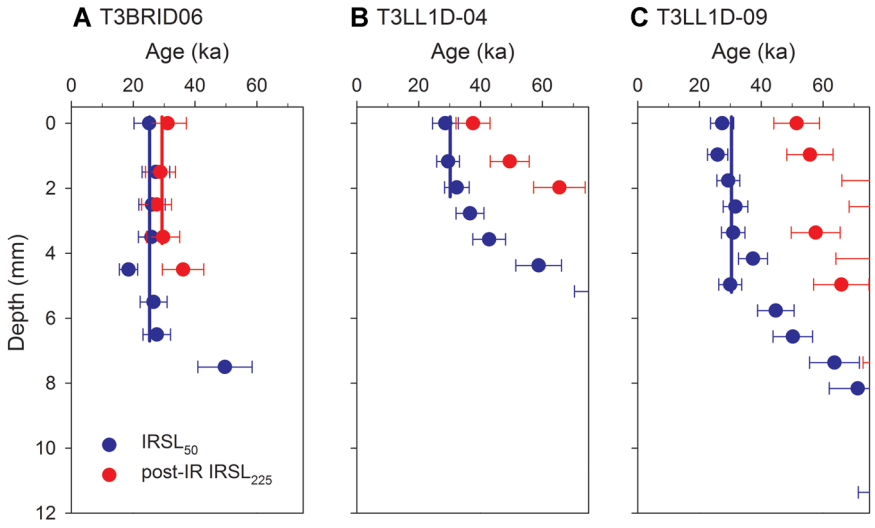

Figure 3 Luminescence ages for three cobbles as a function of depth. The depth to which cobbles were bleached at deposition is shown with vertical solid lines. The same age scale has been used for all three cobbles to aid comparison, and the scale was chosen to show clearly the data which record the most recent exposure to daylight. [Color figure can be viewed at wileyonlinelibrary.com]

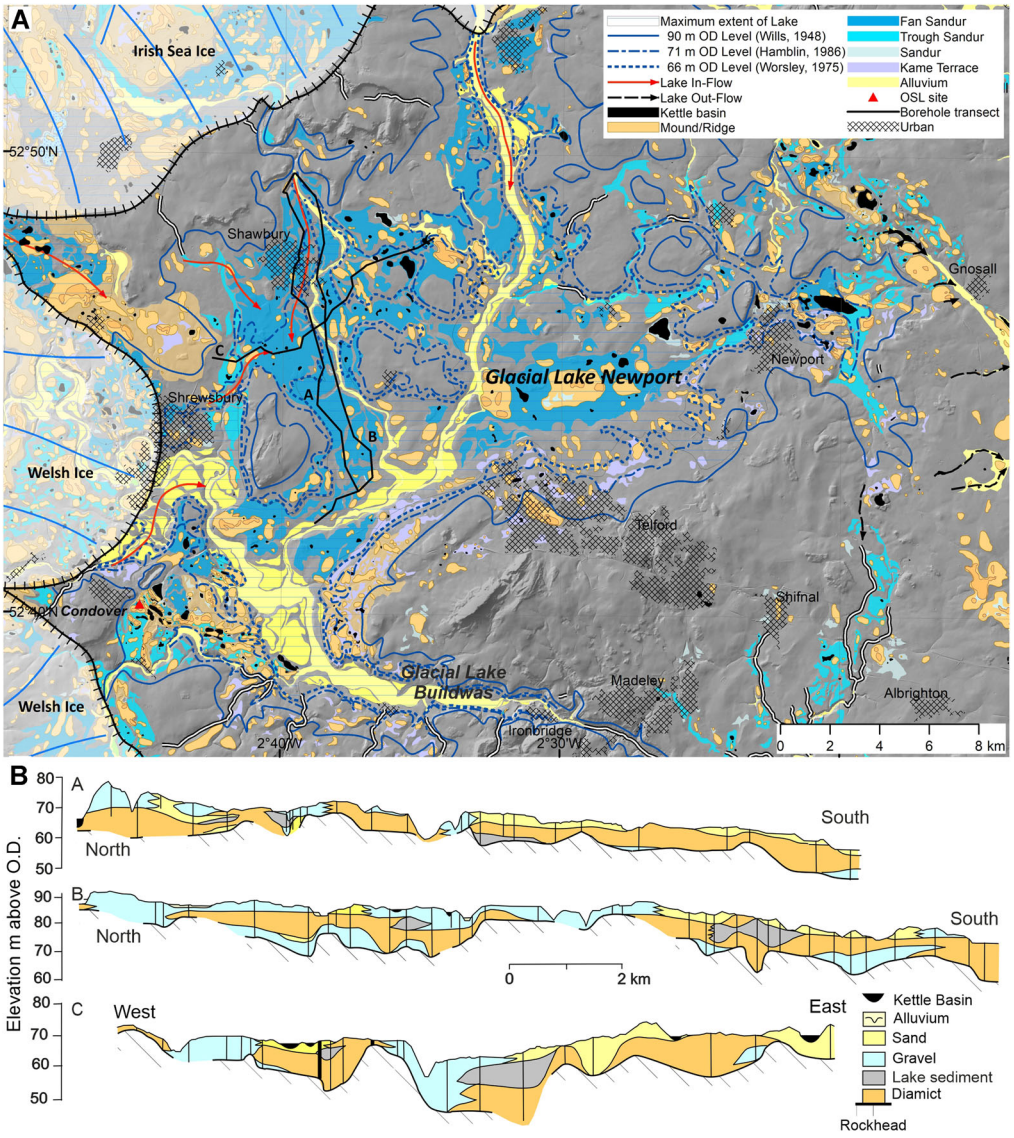

Figure 4. (A) Glacial geomorphology of Glacial Lake Newport, borehole cross-section lines, the former shorelines of the lake (Wills, 1948; Worsley, 1975; Hamblin, 1986) and feeding sandur systems, showing the location of probable former ice margins and Condover Quarry. (B) Borehole cross-sections A, B and C extending into Glacial Lake Newport. [Color figure can be viewed at wileyonlinelibrary.com]

entrenched valleys floored by glacial outwash deposits. Zone 2 is dominated by an extensive basin to the west, with moraines displaying an ENE to WSW orientation (Fig. 1C). The low-lying terrain, palaeo-lake Newport/Buildwas, is floored by laminated to massive muds, sands and gravels, with southward-draining extensive former sandur fans to the north (Zone 4) (Fig. 4) (Whitehead *et al.*, 1928; Wills, 1948). The most extensive moraines and kame terraces occur south of the former lake, to the north of the Wenlock Edge – Wrekin escarpment (Fig. 1C). Palaeo-lake Newport drained southwards via lake overflows towards the Severn Gorge, the headwaters of the Stour and feeding the Trent in eastern England (Fig. 4) (Wills and Dixon, 1924; Wills, 1948). Zone 3 is an extensive low-lying 6–7-km-wide belt of lobate moraines that reflects the dynamics of Welsh ice. The lobate form suggests relatively unconfined flows of ice most likely after the retreat of the ISG (Wills, 1948; Shaw, 1972a, 1972b), but the cross-cutting axes to some of the moraines show some interaction of Irish Sea and Welsh-sourced ice during this deglaciation (Fig. 1C). Between the Welsh readvance moraines and retreating ice margin lies former Glacial Lake Severn, which received outwash from Welsh ice and Irish Sea ice through a fan-delta on its northern shores (Fig. 5) (Wills, 1948).

There are few depositional glacial landforms on the bedrock high (Zone 4), where Carboniferous strata in the east and Permo-Triassic sandstones in the west crop out. Through-valleys dissect these uplands, each former conduits for subglacial and proglacial meltwaters feeding rivers south and eastwards. These over-deepened valleys are the only substantial glacigenic landforms, and are floored with sands and gravels deposited as former glacial outwash sandur that drained southwards to Glacial Lake Prees (Fig. 6) (Thomas, 1989). The ISG climbed an 80–100-m high reverse slope in Zone 5, which preserves an extensive lobate belt of moraines that is widest (14–21 km) in the west and narrower (3–5 km) in the east where the bedrock rises towards the Peak District (Peake, 1961; Poole and Whiteman, 1961; Thomas, 1989; Parkes *et al.*, 2009). Three major ice lobes are reflected in the moraine geometry, and show a planform heavily affected by the bedrock topography. Kettlehole lakes and basins are ubiquitous and form a landform signature of ice stagnation in the west reflecting the widespread abandonment of dead-ice within the moraines during deglaciation (Thomas, 1985a). The kettleholes and associated dead-ice are a less abundant component of the land-system in the east. In Zone 6 low-lying lobate arcuate moraines record the retreat of four major glacial lobes (Fig. 1C), with the mid-Cheshire bedrock ridge a significant regulator of the

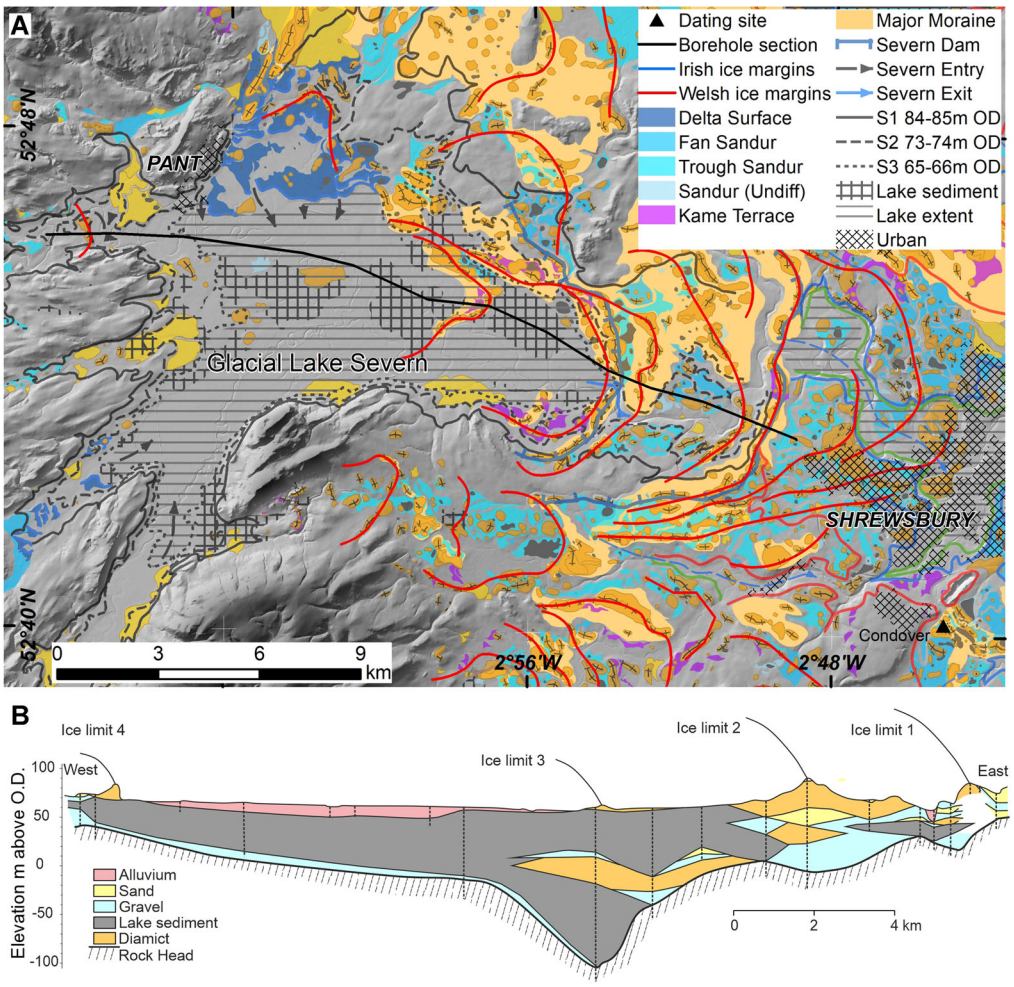

Figure 5. (A) Glacial geomorphology of Glacial Lake Severn (Wills, 1948), borehole cross-section lines, former lake shorelines S1 to S3 and location of Condover Quarry. (B) Borehole cross-section extending across former Glacial Lake Severn. [Color figure can be viewed at wileyonlinelibrary.com]

ice-marginal landform geometry. Proglacial lakes formed between the retreating ice margins and the higher terrain to the south, including Glacial Lake Bangor (Thomas, 1985a, 1989, 2005) and others further east: Glacial Lakes Delamere, Wynbunbury and Congleton (Fig. 1C). Former deltas fronting the ISG margins have left extensive raised terraces formed by glacifluvial waters discharging into the lakes around Wrexham and Delamere (Thomas, 1985a, 1989).

South Lancashire (Zone 7) is dominated by an E–W bedrock high reaching <175 m above the surrounding topography and dissected by NW–SE aligned through-channels (Chiverrell *et al.*, 2016). The largest of these channels are occupied by the Dee and Mersey Estuaries (Longworth, 1985), and they were all incised by subglacial and latterly proglacial meltwaters. Low-amplitude moraines in Zone 8 form two major belts that developed fronting the ISG and eastern Cumbrian ice, with further moraines in the lower Ribble Valley fronting a Ribble Valley Glacier (RVG) (Mitchell, 1991; Mitchell and Hughes, 2012; Chiverrell *et al.*, 2016). The low, sub-parallel ridges of the 'Kirkham Moraine' (Gresswell, 1967; Chiverrell *et al.*, 2016) in Zone 9 are dissected by N–S proglacial channel systems (Fig. 1B), with further arcuate sub-parallel moraine ridges stepping back northwards recording the decline of ice across north Lancashire (Chiverrell *et al.*, 2016).

Marginal limits and dynamics

Subglacial bedforms are scarce across the region and so ice flow patterns have been interpreted from the very well-developed moraine record (Fig. 1B). These former ice margins have been subdivided based on the ice source areas, distinguishing the ISG from tributary ice masses sourced from Wales, eastern Cumbria and the Pennines. Major and minor ice-marginal positions were discerned from interpretation of moraine ridge continuity and geometry, with larger and more continuous ridges interpreted as major ice limits and smaller, less continuous ridges forming minor ice limits (Fig. 1B). Major suites of ridges have been identified as ice-marginal limits (L1–9) and interpreted in terms of readvance, oscillation or stand-still of the ISG margins. These limit positions (L1–9: Fig. 1B) have guided our selection of sites for geochronological analysis.

Maximum ice limits are reflected in sporadic moraines, and their small scale and the limited accumulation of proglacial sediments suggests that this advance (L1: Fig. 1B) was either short-lived or not particularly erosive and with no significant still-stand or readvance during subsequent retreat (Fig. 1C). Sediment transport pathways to Zone 1 had to overcome the Wenlock Edge – Wrekin ridge with the main outwash conduit through the Severn Gorge. Ice-marginal moraines and kame terraces with a strong E–W continuity occur north of the Wenlock Edge – Wrekin ridge (L2: Fig. 1C), alongside other minor limits also reflecting an E–W configuration. Stepping northwards towards Zone 4 indications of former ice limits are well defined (L3: Fig. 1C), particularly along the Zone 2–3 boundary where Welsh ice moraines are prevalent. These moraines record the step back of the Severn Valley Glacier (SVG) into Wales with a series of arcuate major limits (Fig. 1C). To the north the SVG was constrained by the presence of the ISG, but further south Welsh

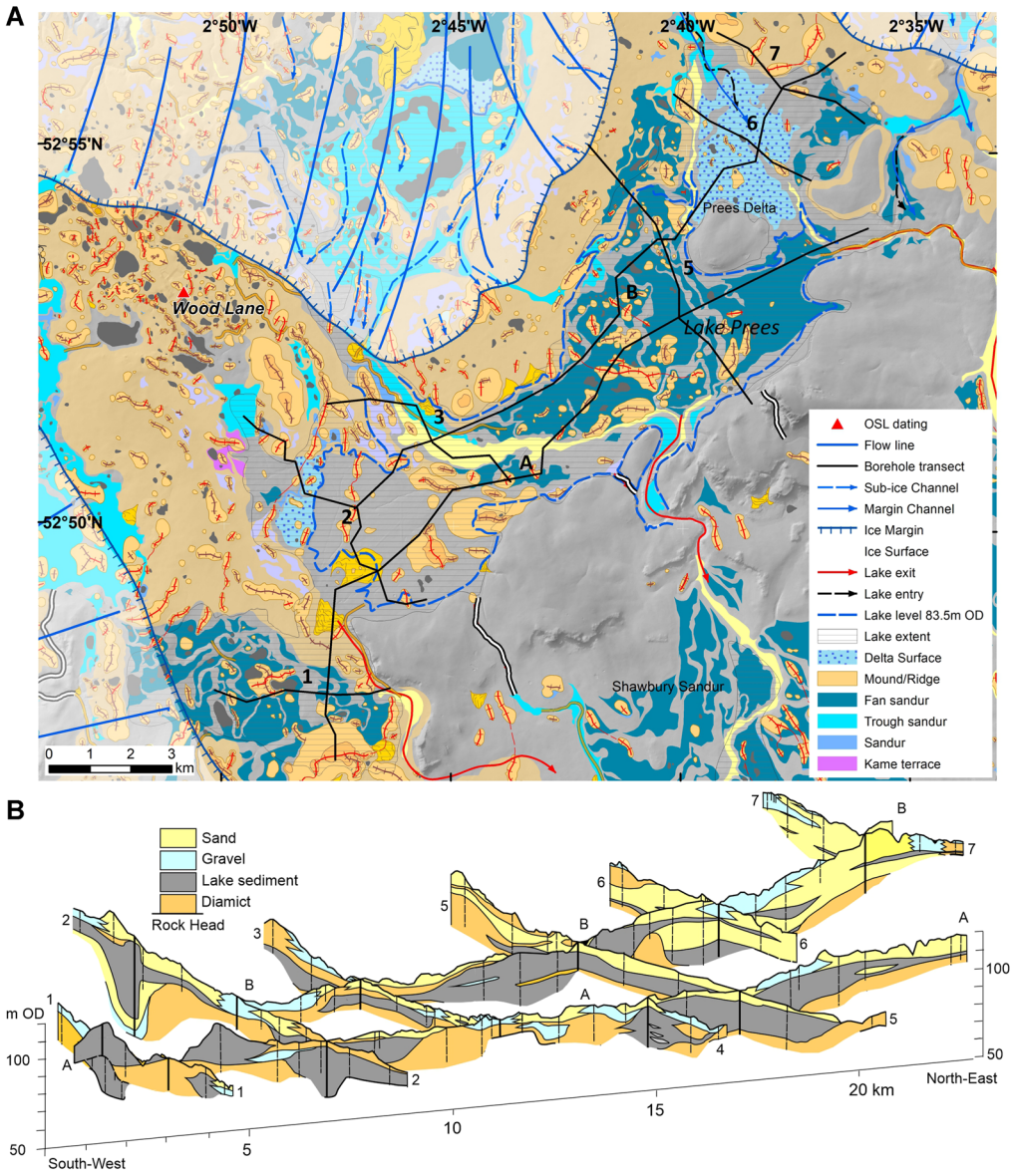

Figure 6. (A) Glacial geomorphology and borehole cross-section lines of former Glacial Lake Prees, showing the location of probable former ice margins and Wood Lane Quarry in the Oswestry–Whitchurch–Congleton moraine. (B) Borehole cross-section fence sections extending into Glacial Lake Prees. [Color figure can be viewed at wileyonlinelibrary.com]

ice was unimpeded and extended as a lobate form (Shaw, 1972a, 1972b). Former Glacial Lake Severn is largely devoid of moraines (Fig. 5), but this may in part reflect burial beneath thick accumulations of lake sediment.

Fronting at least four ISG lobes, the largest moraine complex in the region (L4–5: Fig. 1C) is compound and comprises multiple ridges. Some of the morphological complexity reflects ice stagnation and disintegration, with ice compressional stresses against a reverse slope encouraging potentially more supraglacial debris to be deposited and then ice stagnation leaving extensive dead-ice buried within the deposits. Further east, the moraines contain fewer kettleholes and geophysical investigations have shown glacitectonism and a more active ice margin in the glacial deposits (Parkes *et al.*, 2009). Thus, variations in the ice-marginal dynamics occurred along the 100-km ice front and between the ice lobes (L4–L5: Fig. 1C). Progressing northwards from L4 to L5 the moraines are typically subdued and often buried by substantial accumulations of outwash and glacilacustrine sediment. In places the moraines are more prominent, for example the well-developed ice-marginal moraine system bordering Wales (Thomas, 1985a). The most substantial depositional landforms are the delta terraces around Wrexham in the west (Thomas, 1985a) and Delamere east of the mid-Cheshire ridge. The ice contact slopes to the rear of both deltas were major still-stands of the ice margin (L6: Fig. 1C) during which outwash sands and gravels entered former glacial lake basins.

A series of ice-marginal still-stands has formed a belt of moraines and kames (L7: Fig. 1B) along the break in gradient as ice pulled back into south Lancashire (Chiverrell *et al.*, 2016). Climbing bedrock slopes northwards, these moraines reduce in size and are widely spaced perhaps reflecting more rapid ice retreat (Chiverrell *et al.*, 2016). L8 (Fig. 1B) describes a belt of ice-marginal kames and moraines and reflect the pull-back of ice generating a major limit as ISG and Cumbrian ice margins retreated and the ice masses decoupled, including the Tarleton and Chorley moraines (Price, 1963; Chiverrell *et al.*, 2016). The moraine geometry reflects this decoupling, with moving northwards the ISG moraines increasingly either subdued or now offshore (Chiverrell *et al.*, 2016). The ice-marginal geometries show the interaction of ISG and Cumbrian ice with a confluent RVG. North of the Ribble Valley there is the second largest moraine system (L9: Fig. 1B) in the region, the Kirkham Moraine, a belt of ridges separated by marginal

sandur systems (see Chiverrell *et al.*, 2016). The configuration of the L9 moraine was associated with advance of Cumbrian ice at a time when ISG was still present to the west. Repeated still-stand and short-distance oscillation of the margin is associated with the formation of L9 and during subsequent retreat northwards (Chiverrell *et al.*, 2016).

Glacial lakes of the English Midlands

Glacial lakes have long been postulated in the Cheshire–Shropshire lowlands (Wills and Dixon, 1924; Wills, 1948; Worsley, 1975), and debates about their existence and extent are bound to the concept of the classical 'Lake Lapworth' (Wills and Dixon, 1924). Refining understanding of glacial lakes in Cheshire–Shropshire has been through several iterations (Worsley, 1975; Thomas, 1985a, 1989; Worsley, 2005; Murton and Murton, 2012), and includes the interpretation of former glacial lake environments at Prees, in the Dee and Severn Valleys, and in the major L4–L5 and L9 moraine complexes (Fig. 1B). The lack of continuity to their sedimentary record led to them being regarded as small, irregular and unconnected pro- and sub-glacial lakes rather than major regional lakes (Cannell and Harries, 1981; Cannell, 1982; Wilson *et al.*, 1982). The topography provides more restricted opportunity for the development of proglacial lakes in the south, for example Glacial Lake Morville (Wills and Dixon, 1924) forming between ISG ice margins and the Wenlock Edge bedrock escarpment (Fig. 7). This small and temporary proglacial lake was ponded between a N–S aligned ice margin and bedrock slopes to the west. The sediment–landform signature and geochronology of Glacial Lake Morville has been developed using exposures at Bridgwalton Quarry (Fig. 7).

Upstream of Ironbridge Gorge (Fig. 4A), more widespread flat ground floored by glacilacustrine sediments evidence an extensive glacial lake, including deltaic ice-proximal deposits that have been attributed to Lake Buildwas and Lake Newport (Wills and Dixon, 1924; Shaw, 1972a, 1972b). Lake Buildwas drained south to the Severn through Ironbridge Gorge and Lake Newport eastwards to the Trent at Gnosall (Fig. 4A), but with ice-marginal retreat these lakes merged and meltwater discharge was solely focused through Ironbridge Gorge and the River Severn (Wills and Dixon, 1924; Wills, 1948; Worsley, 1975). This lake is heavily associated with both the 'Lake Lapworth' concept (Wills and Dixon, 1924; Poole and Whiteman, 1961; Worsley, 1975; Thomas, 1989) and the dynamic evolution of drainage thresholds associated with the incision or re-excavation of Ironbridge Gorge. The sediment–landform record is equally complicated, showing a mixture of glacilacustrine silts/clays, outwash sands and gravels, and glacial diamicts. Former quarry exposures at Buildwas, near Ironbridge (Fig. 4A) (Wills and Dixon, 1924), showed 30 m of laminated glacilacustrine muds, including diamict blocks interpreted as dropped from floating icebergs, overlain by diamict, outwash gravels and sands near the entry to Ironbridge Gorge. Borehole transects (Fig. 4B), from the centre of the Lake Newport basin northwards, show <20 m thickness of spatially variable glacigenic sediments overlying bedrock (Hamblin, 1986), with diamictons interspersed with sporadic glacilacustrine muds and a dominance of glacifluvial sands and gravels to the north prograding into the lake basin (Fig. 4). Glacial Lake Newport developed as a relatively shallow basin (30–20 m water depths) and evolved with the retreat of the ice margins. Supraglacial debris and widespread abandonment of dead-ice with retreat of the ice margins is reflected in the kettleholes ubiquitous across the lake floor. The sediment–landform assemblages present a model of relatively shallow and time transgressive lakes, with shallowing driven by a combination of base level incision at Ironbridge and basin infill (Fig. 4B). Further west, the borehole stratigraphy underlying Glacial Lake Severn (Figs 1C and 5) shows thick accumulations of glacilacustrine sediment that evidence a substantial over-deepening terminating at the confluence of Welsh and ISG ice. The basin is filled predominantly by glacilacustrine muds (Fig. 5B), descends >75 m below present sea level and is bounded in the east by the rising rock-head and Welsh readvance moraines (Fig. 5A). The scale of over-deepening (>170 m depth and dimensions of 19 × 6 km) is intriguing and not a feature of the regions' other former glacial lakes. The sediment fill and process of over-deepening may span more than one glacial cycle, but compressional stresses generated as Welsh ice collided with the ISG compounded by the rising rock-head offer a mechanism for generating intense basal scour and over-deepening. Condover Quarry lies between Glacial Lakes Newport and Severn (Figs 4A and 5A), and the exposures were sampled to date the ice margins associated with these proglacial lake basins and the readvance of Welsh ice.

Glacial Lake Prees (Thomas, 1989) was a lengthy and narrow (20 × 5 km) ice-marginal lake that formed between the L4–L5 ice margin feeding ISG outwash and the Triassic bedrock escarpment to the south (Zone 4: Fig. 6A). Borehole transects show that the lake was divided into separate basins by diamict ridges (Fig. 6B), and these lakes were probably in existence at different times. Lake sediment thicknesses reach 25 m in the deeper (40–30 m water depths) basin and are commonly intercalated with diamict and outwash sands and gravels. Packages of diamict, overlain by outwash sands and gravels, dominate the northern margins of the lake lain down initially by ice-contact lacustrine processes and latterly by proglacial outwash prograding into the basin (Fig. 6B). Changes in sediment compositions between adjacent boreholes occur over short distances and reflect the dynamic nature of the glacilacustrine sub-environment. Glacial Lake Prees developed as an ice-contact system but became proglacial as the ice margins withdrew towards the L4–L5 moraine (Fig. 6). As the ice margins retreated, prograding deltaic and sandur sediments filled the basin. Ultimately, Glacial Lake Prees decoupled from the ISG with ice-marginal retreat northwards (Thomas, 1985a; Thomas, 1989), and set inside the L4–L5 moraines further more extensive proglacial lakes developed in the lower Dee and Weaver basins (Fig. 1C). Wood Lane Quarry, near Ellesmere, lies immediately north of Glacial Lake Prees (Fig. 6A), and the exposures were sampled to constrain both retreat from the lake basin and the development of the L4–L5 moraine complex (see 'Zone 5' below).

Glacial Lakes Bangor (Thomas, 1989) and Delamere formed as proglacial basins as the ice margins retreated further north developing a series of ice-marginal moraines (Fig. 1C). Extensive deltas form the western margins of Glacial Lakes Bangor (Thomas, 1989) and Delamere. Based on the height of delta top-sets exposed in the Wrexham Delta at Borras Quarry (Thomas *et al.*, 1985), Glacial Lake Bangor was at its maximum 10 km wide and 30 km long, had a maximum lake level of 70 m OD and waters <70–80 m deep were ponded against the L4–L5 moraines and bedrock slope. Glacial Lake Delamere was one of a series of smaller lakes that developed in the Weaver basin with north-westward retreat of the ice margins. The delta complex on the western margins around Delamere had a surface elevation of 85–75 m and water depths probably of 40–60 m. The basin sediments comprise a thick sequence of

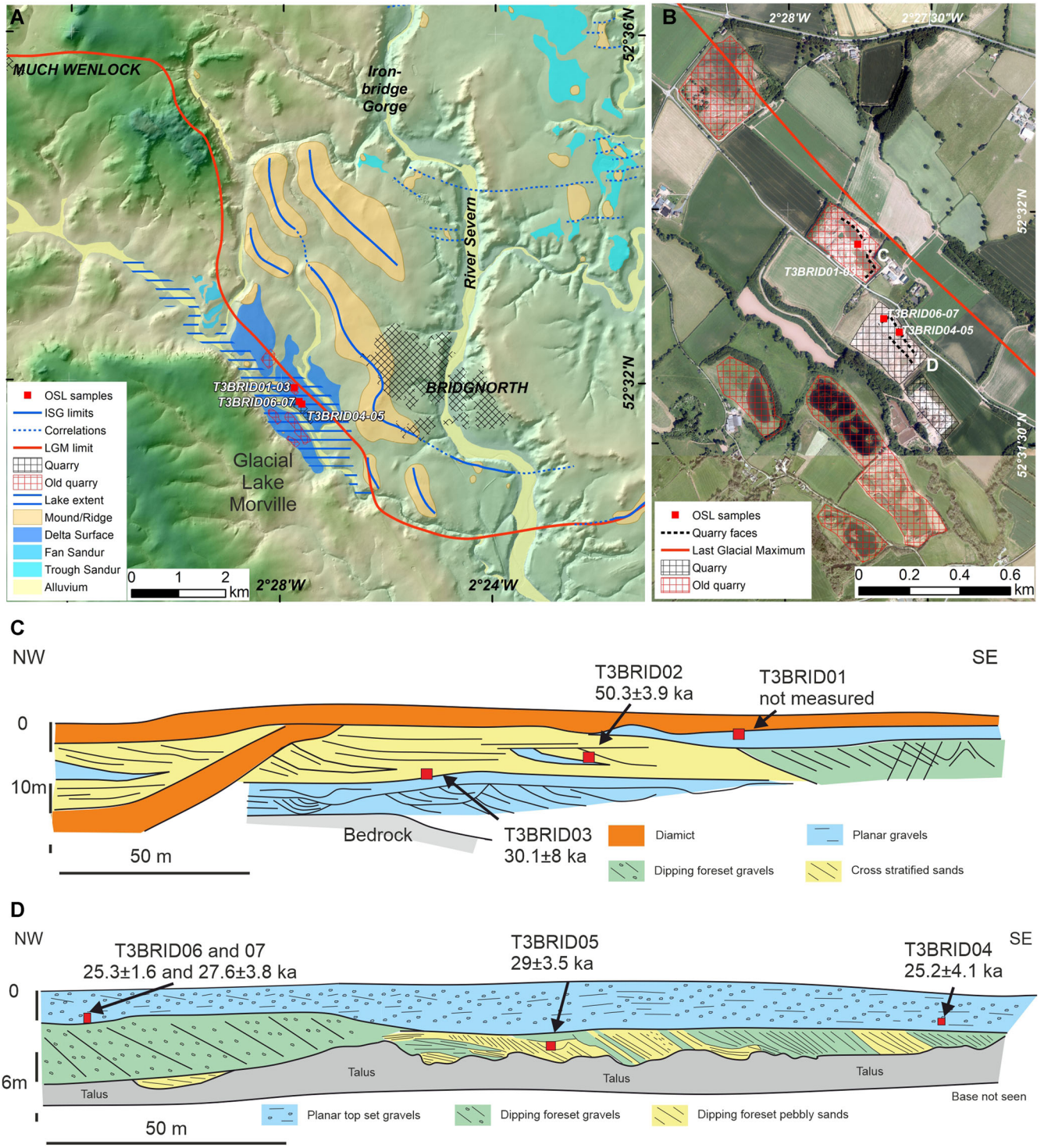

Figure 7. (A) Glacial geomorphology of the Mor Brook valley and Glacial Lake Morville at the maximum extent of the Irish Sea Glacier (ISG). (B) Quarry exposures at Bridgwalton showing the locations of the described faces and sampling locations (© Getmapping PLC Aerial EDINA Digimap). (C) Exposures inspected May 2013 and the locations and ages obtained for samples T3BRID01-03. (D) Exposures inspected May 2014 to August 2017 and the locations and ages obtained for T3BRID04-07. [Color figure can be viewed at wileyonlinelibrary.com]

lacustrine muds, sands and gravels, which are well exposed owing to several decades of sand and gravel extraction at multiple quarries in the area. Sediment exposures at Borras Quarry (Lake Bangor) and Cherry Orchard Farm (Lake Delamere) were sampled to constrain the L6 ice margins associated with the deltas prograding into these lake basins (see 'Zone 6' below).

The topography fronting the retreat of ice margins northwards through Zone 7 is less conducive to the development of proglacial lakes, but between ice limits L8 and L9 temporary lakes developed in front of the retreating ice margins and in the lower Ribble Valley (Fig. 1B) (Earp *et al.*, 1961; Aitkenhead *et al.*, 1992; Chiverrell *et al.*, 2016). The retreat of Cumbrian and RVG ice produced a proglacial lake ponded to the west by the ISG (Chiverrell *et al.*, 2016), and this expanded eastwards with retreat of RVG ice margins up the Ribble Valley (Earp *et al.*, 1961; Aitkenhead *et al.*, 1992). Sediment exposures at Lydiate Lane Quarry (L8 ice margin) and Bradley's Sandpit (L9 ice margin) (Fig. 1B) were sampled principally to constrain these former ice marginal configurations and bracket the development of proglacial lakes in the lower Ribble Valley (see 'Zones 8 and 9' below).

Sedimentology and geochronology

Zone 1: maximum ice limits in the English Midlands

The maximum extent achieved by the ISG in the English Midlands impinged on a small tributary (Mor Brook) of the River Severn south of Ironbridge Gorge near Bridgnorth (Fig. 1C). East of Mor Brook (Fig. 7) there are low-relief ridges composed of glacial diamict that mark the maximum limit of ice advance. Thick accumulations of outwash sands and gravels have accumulated in the valley in front of this ice limit as ISG ice blocked the valley creating a small ice-dammed lake, Glacial Lake Morville (Fig. 7A). The sand and gravel deposits associated with Glacial Lake Morville have been exploited as mineral aggregate for > 50 years. Decades of sand and gravel extraction at Bridgwalton Quarry have shown a > 15-m sequence of sands and gravels overlying bedrock (Fig. 7B), in which low-angle stacked packages of planar and trough cross-stratified gravels become more sand dominated towards the surface (Fig. 7C). Development of the quarry has progressed from ice-proximal exposures in 2013 (Fig. 7C) more or less contiguously to ice-distal exposures in 2014–2017 (Fig. 7D). Together the stratigraphical sections are dominated by low-angle (~20°) delta fore-set sands and gravels dipping and thickening towards the south-east and these are overlain by <2 m of planar massive stratified delta top-set gravels. Throughout the sequence, palaeocurrent evidence indicates flows to the south. The stratified medium–coarse sandier units contain granule to pebble gravels and frequent out-sized clasts (Fig. 7C) and are interpreted as typical of delta fore-set beds deposited as cohesionless debris-flows down the delta front into a shallow lake (Smith and Ashley, 1985; Nemec *et al.*, 1999; Nemec, 2009). The outsized clasts may either be drop-stones or gravity-fed debris rolling down the delta front. The upper 3–2 m (Fig. 7C) comprises planar massive stratified gravels (Gms) with occasional planar cross-stratified gravels (Gp) and pockets of sands (Sh and Sp) becoming gravel dominated with proximity to the former ice margin. Locally, a thin (~2 m) diamicton caps the more ice-proximal sections (Fig. 7C), whereas the more ice-distal exposures showed no evidence of this diamicton; it probably reflects a small-scale advance of ice onto the outwash surface. To the south-east, the uppermost planar geometry sheet of laminated gravel and medium-coarse sand (Sh) with some fine laminations (Fl) becomes thicker and is interpreted as a delta top-set (Fig. 7D).

Samples T3BRID02 and T3BRID03 were taken in 2013 from back bar sands in an ice-proximal delta top-set and sampled rippled medium sands (Sr) within planar cross-stratified sands (Sp). In April 2014, new exposures of the more ice-distal delta top-sets allowed for sampling of planar geometry sheet laminated medium–coarse sand (Sh) with some fine laminations (Fl) (T3BRID04) and sheet laminated medium sand (Sh) at the fore-set to top-set transition (T3BRID05). These distal exposures were revisited in August 2017 showing a gravel-dominated upper 2–3 m of the delta top-set, which were sampled collecting ~20 cobble-sized granites and an adjacent sand sample (T3BRID07) was taken from a channel fill in the top-set gravels. SA-OSL analyses focused on four samples (T3BRID02-05). The asymmetrical D_e distributions determined for T3BRID02 and T3BRID03 (Fig. 2A) suggest that these samples were bleached heterogeneously before burial, where a small proportion of the grains characterize the minimum dose population due to limited exposure to sunlight before burial. The D_e distributions determined for T3BRID04 and T3BRID05 (Fig. 2A) were also asymmetrical and therefore heterogeneously bleached before burial. However, the minimum dose populations in the D_e distributions for T3BRID04 and T3BRID05 contained a greater proportion of the grains than those determined for samples T3BRID02 and T3BRID03 (Fig. 2A). T3BRID02 and T3BRID03 were taken from ice-proximal settings with diamictons bedded within and capping the sequence, which suggests relatively short sediment transport distances, with T3BRID04 and T3BRID05 from more ice-distal settings within the delta (Fig. 6D). Samples T3BRID06-07 were taken from the same section as T3BRID04-05, but from more ice-proximal and coarser grained lithofacies. The single-grain D_e distributions determined from quartz grains of sample T3BRID07 were asymmetrical and therefore the grains were also heterogeneously bleached before burial. Age–depth profiles determined for the cobble (BWT03-1: T3BRID06) confirm that the outermost parts were well-bleached, with low $IRSL_{50}$ and post-IR $IRSL_{225}$ L_n/T_n ratios at the surface gradually increasing at a depth of ~ 6 mm. $IRSL_{50}$ ages are consistent to a depth of ~ 7 mm and this supports the interpretation that the cobble had been well-bleached at deposition (Fig. 3).

Seisdon Quarry (Fig. 1C) is located 16 km further east of Bridgwalton and is part of a series of quarries that have exploited the Trysull sands and gravels for >70 years (Morgan, 1973). The bulk of the stratigraphy at the Trysull–Seisdon quarries spans several marine isotope stages (MIS) including interglacial units, but the uppermost glaci-fluvial outwash sand and gravels containing Irish Sea erratics are unconformable on a cryoturbated palaeo-land surface and potentially date to the last glaciation (Morgan, 1973). The exposures in November 2012 revealed ~10 m of these uppermost orange stratified sands, and two adjacent samples were taken for OSL dating (T3SEIS01 and T3SEIS02) to constrain the timing of the ISG impinging on the River Stour basin within 3 km of the LGM limit south of Wolverhampton (Fig. 1C). Both samples were horizontally laminated sand (Sh) lithofacies within a channel fill. Asymmetrical D_e distributions (Fig. 2B) determined by parallel SA-OSL and SG-OSL suggest that both samples were bleached heterogeneously before burial, and only a small proportion of the grains characterize the minimum dose population probably because of limited exposure to sunlight before burial.

The ice-marginal position at Bridgwalton constrains the maximum extent of ice in the English Midlands (L1: Fig. 1C). The SA-OSL age determined for T3BRID02 of 50.3 ± 3.9 ka is considered an inaccurate estimate of the time of deposition reflecting poor bleaching of the OSL signal. Therefore, the maximum ice limit at Bridgwalton was constrained by the SA-OSL ages of 25.2 ± 4.1 ka (T3BRID04) and 29.0 ± 3.5 ka (T3BRID05), alongside SG-OSL ages of 30.1 ± 8 ka (T3BRID03) and 27.6 ± 3.8 ka (T3BRID07). The cobble (T3BRID06) yielded an age of 25.3 ± 1.6 ka. The geochronology from Seisdon is equivocal, with T3SEIS02 yielding an SG-OSL age of 48.8 ± 8.4 ka, different to the SA-OSL age 22.9 ± 3.4 ka for the same sample. T3SEIS01 also measured for SG-OSL yielded an age of 58 ± 8.3 ka. The two SG-OSL ages overlap within uncertainties and pre-date MIS 2, whereas the SA-OSL age for T3SEIS01 is ~26 ka younger than the paired single grain measurement. It is unclear why the SA-OSL approach should recover a younger minimum dose population than equivalent single grain measurements for the same materials.

Zone 2: Glacial Lakes Newport and Severn

After the retreat of the ISG margins northwards, a readvance by Welsh ice produced a series of lobate moraines that extend as far east as Shrewsbury. These moraines form the boundary between former Glacial Lakes Newport and Severn (Figs 1C, 4 and 5). The sand and gravel workings at Condover have

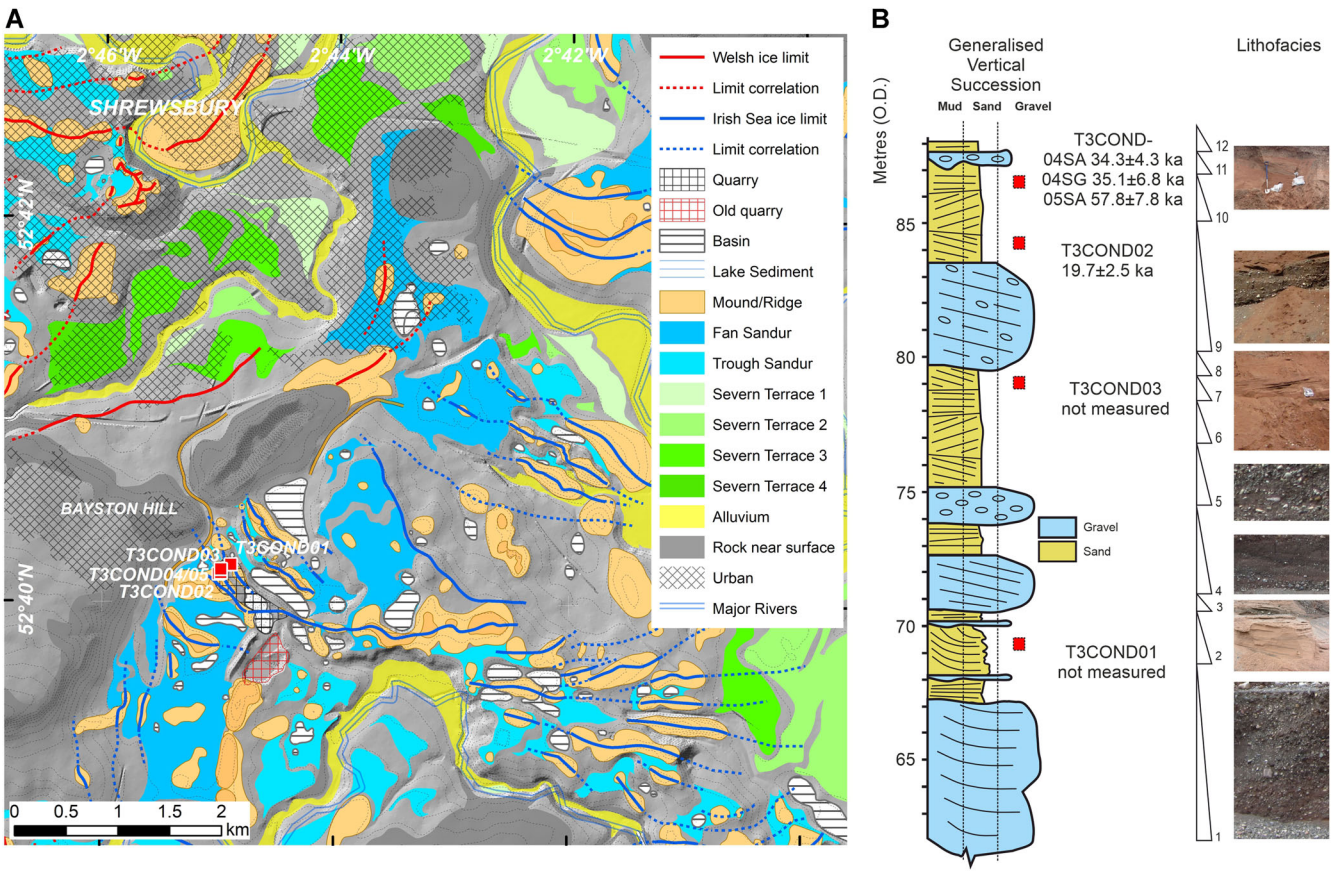

Figure 8. (A) Glacial geomorphology of the Condover Quarry region. (B) Generalized vertical succession of the 2013–2017 exposures, the locations and ages obtained for samples T3COND01-05 and associated lithofacies photographs. [Color figure can be viewed at wileyonlinelibrary.com]

exploited a sandur fan issuing from gaps in a Precambrian bedrock ridge into a basin south of Bayston Hill (Fig. 8). A series of E–W aligned moraine ridges show Irish Sea ice rode over this ridge, but SW–NE orientated ridges show a Welsh readvance extending to the ridge crest (Figs 5 and 8A). The quarry workings were limited to steps of 2–3 m in height, and so the vertical sequence was compiled from multiple short-lived exposures (2014–2016). The generalized vertical succession recorded for the quarry revealed repeating cycles of bar-form massive (Gm) or trough cross-stratified channel (Gt) gravels fining upwards into back-bar parallel-laminated sands (Sh) and planar cross-bedded units (Gp and Sp) (Fig. 8A). The sequence is typical of variable high-discharge and high-energy units, which were probably adjacent to the ice margins given the occasional diamictons elsewhere in the quarry and the extensive post-depositional faulting and numerous kettle basins (Scourse *et al.*, 2009) caused by the melt-out of dead-ice. OSL dating of the sequence has focused on the uppermost 5–8 m and the most recent phase of outwash deposition related probably to the readvance of Welsh ice. T3COND02 sampled cross-stratified back-bar or channel fill sands, whereas T3COND04 and T3COND05 sampled horizontal sheet laminated medium sands between back-bar planar cross-stratified sands (Sp). The D_e distributions determined for all the samples were asymmetrically distributed (Fig. 2C), which indicates that the sediment was heterogeneously bleached before burial. The geochronology from the uppermost units is equivocal, with T3COND04 yielding paired SG-OSL and SA-OSL ages for the same sample of 35.1 ± 6.8 and 34.3 ± 4.3 ka, respectively, which overlap within uncertainties, but they are younger than the SA-OSL determination of 57.8 ± 7.8 ka measured for the adjacent T3COND05 sample. T3COND02 ~3–4 m lower in the sequence was also measured for SA-OSL yielding an age of 19.7 ± 2.5 ka. The older age determinations (T3COND04 and 05) are geologically implausible, pre-dating the advance to maximum limits evidenced further south at Bridgwalton. The age of 19.7 ± 2.5 ka (T3COND02), although overlapping within the uncertainties, is slightly younger than the cluster of ages from Wood Lane Quarry documenting the retreat of the ISG northwards to L4 (Fig. 1B). However, the T3COND02 result provides potentially the first age estimation for the readvance of Welsh ice late during deglaciation and in that context the deposits at Condover and Wood Lane plausibly could be of similar age. T3COND04 and T3COND05 appear to be clear outliers, but T3COND02 is a good fit constraining the readvance of Welsh ice to ~19.7 ± 2.5 ka (Fig. 7B) and the establishment of Glacial Lake Severn in the period after 19.7 ± 2.5 ka (L3–4: Fig. 1B).

Zone 5: the Oswestry–Whitchurch–Congleton moraine

The largest ice-marginal glacigenic feature in the region is the Oswestry–Whitchurch–Congleton moraine complex (Thomas, 1985a, 1989, 2005), which is classified here as the L4 ISG marginal position (Fig. 1B). The L4 margin was reached after the ISG pulled back from Glacial Lake Prees, and subsequent retreat northwards led to the establishment of large proglacial lakes in the lower River Dee and Weaver basins (Fig. 1C). The geomorphology of the Oswestry–Whitchurch–Congleton moraine is complex and riddled with hollows and lakes formed by the melt-out of dead-ice leaving a chaotic and gently undulating ice disintegration terrain (Fig. 9A) (Shaw, 1972a; Thomas, 1985a, 1989, 2005). The only substantial exposures in the moraine are at Wood Lane Quarry (Fig. 9), with the stratigraphy first described in the 1960s encountering two glacial diamictons that interdigitated with outwash sands and gravels (Shaw, 1972a). The recent exposures

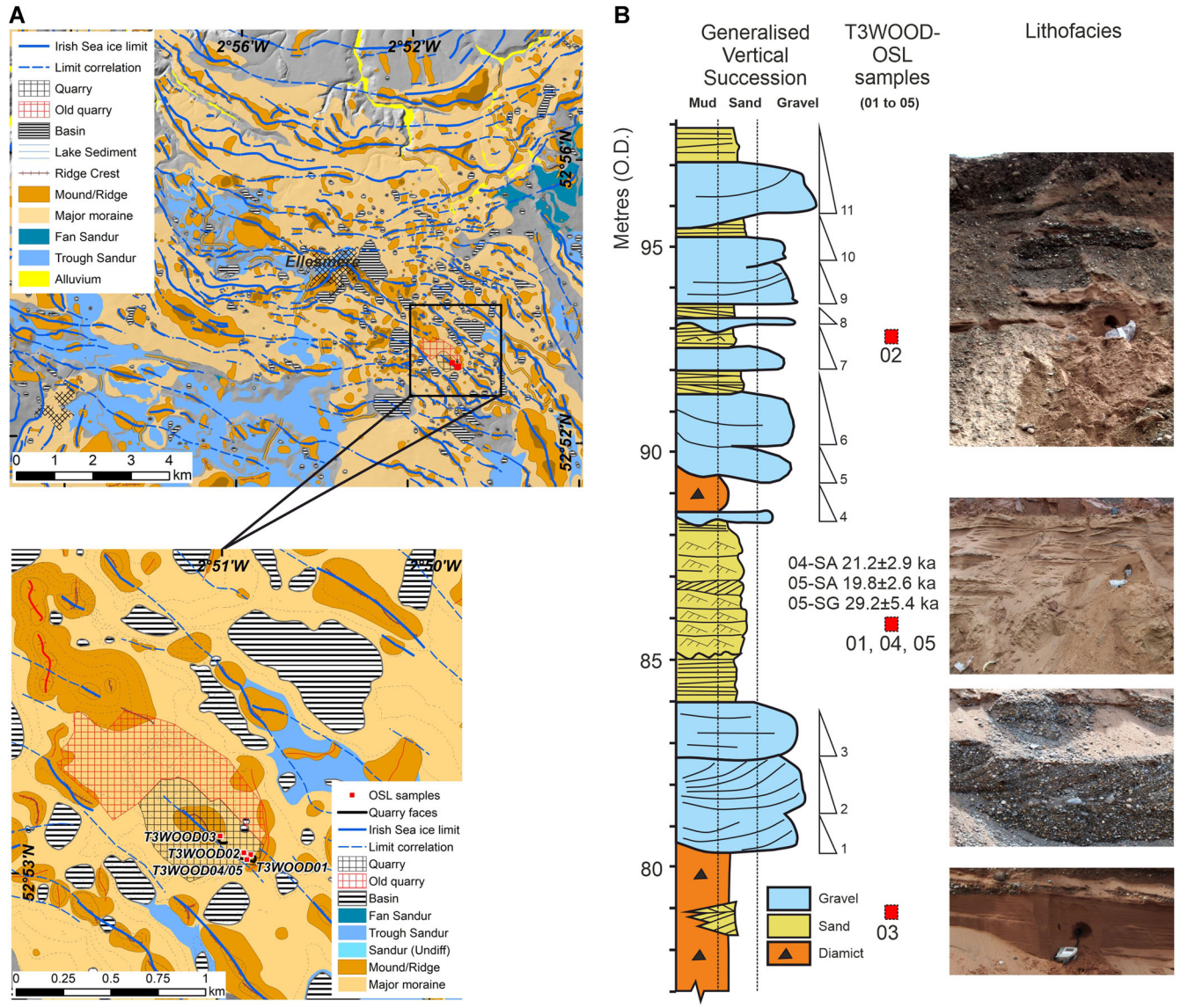

Figure 9. (A) Glacial geomorphology of Wood Lake Quarry region. (B) Generalized vertical succession of the 2013–2017 exposures, the locations and ages obtained for samples T3WOOD01-05 and associated lithofacies photographs. [Color figure can be viewed at wileyonlinelibrary.com]

suggest that aggregate extraction may have removed the upper till as overburden and the vertical sequence 2014–2018 was compiled from multiple sections with aggregate extraction limited to steps of 2–3 m in height through the deposit. A generalized vertical succession (Fig. 9B) shows a laterally discontinuous 2–3-m basal reddish sandy lower diamicton of Irish Sea origin that is interspersed with equivalently red outwash sands and gravels. A 3–4-m-thick sequence of trough cross-stratified and planar outwash gravels overlies the lower diamicton, and is interpreted as probable high-energy channel-fill and associated bar-forms that have a more Welsh lithological origin while still relatively rich with Irish Sea erratic clasts. Overlying the gravels is 4.5 m of medium sands including horizontally stratified (Sh), planar cross-stratified (Sp) and rippled (Sr) facies typical of ice-distal proglacial outwash (Fig. 9B). From this unit T3WOOD04 sampled horizontally stratified medium sands and T3WOOD05 more reddish rippled medium sands. The only differences in material were the reddish character to the T3WOOD05 sands, even though the samples were within 0.5 m of each other. The colour reflects dilution of the typically reddish ISG sediments with grey materials of Welsh provenance, and in the sections, there are locally units with a more red and grey character. The sands are capped variably by thin gravels and a 1-m-thick weakly consolidated sandy diamicton of Irish Sea Ice origin interpreted as an ice-proximal debris flow into a proglacial lake basin. The diamict is overlain by <9 m of fining-upwards cycles (cycles 4–11: Fig. 9B) of massive stratified or cross-stratified gravels (Gt and Gms) grading to horizontally bedded, planar cross-stratified (Sp) and rippled sands (Sr) reflecting migration of channels and bars within an active sandur. Faulting and tectonic structures related to collapse and subsidence support the geomorphological evidence for endemic persistence and then melt-out of dead-ice buried within the deposits. T3WOOD04 and T3WOOD05 both display heterogeneously bleached D_e distributions (Fig. 2D), which reflect poor re-setting of the OSL signal. The stratigraphy suggests this was an ice-proximal high-energy outwash sequence interspersed with overbank or back bar deposits, providing sediment transport distances limiting opportunity for resetting of the OSL signal. Abanico plots of the SA-OSL D_e distributions show a minimum age population is present comprising better bleached quartz and was better resolved for T3WOOD04 with an age of 21.2 ± 2.9 ka (Fig. 2D). T3WOOD05 underwent parallel SA-OSL and SG-OSL analysis. The SA-OSL analysis returned a similar minimum D_e population, and age 19.8 ± 2.6 ka, as T3WOOD04. The SG-OSL measurements of T3WOOD05 gave an older age (29.2 ± 5.4 ka), although this overlaps at two standard deviations (Fig. 2D; Table 2). The OSL ages for samples T3WOOD04

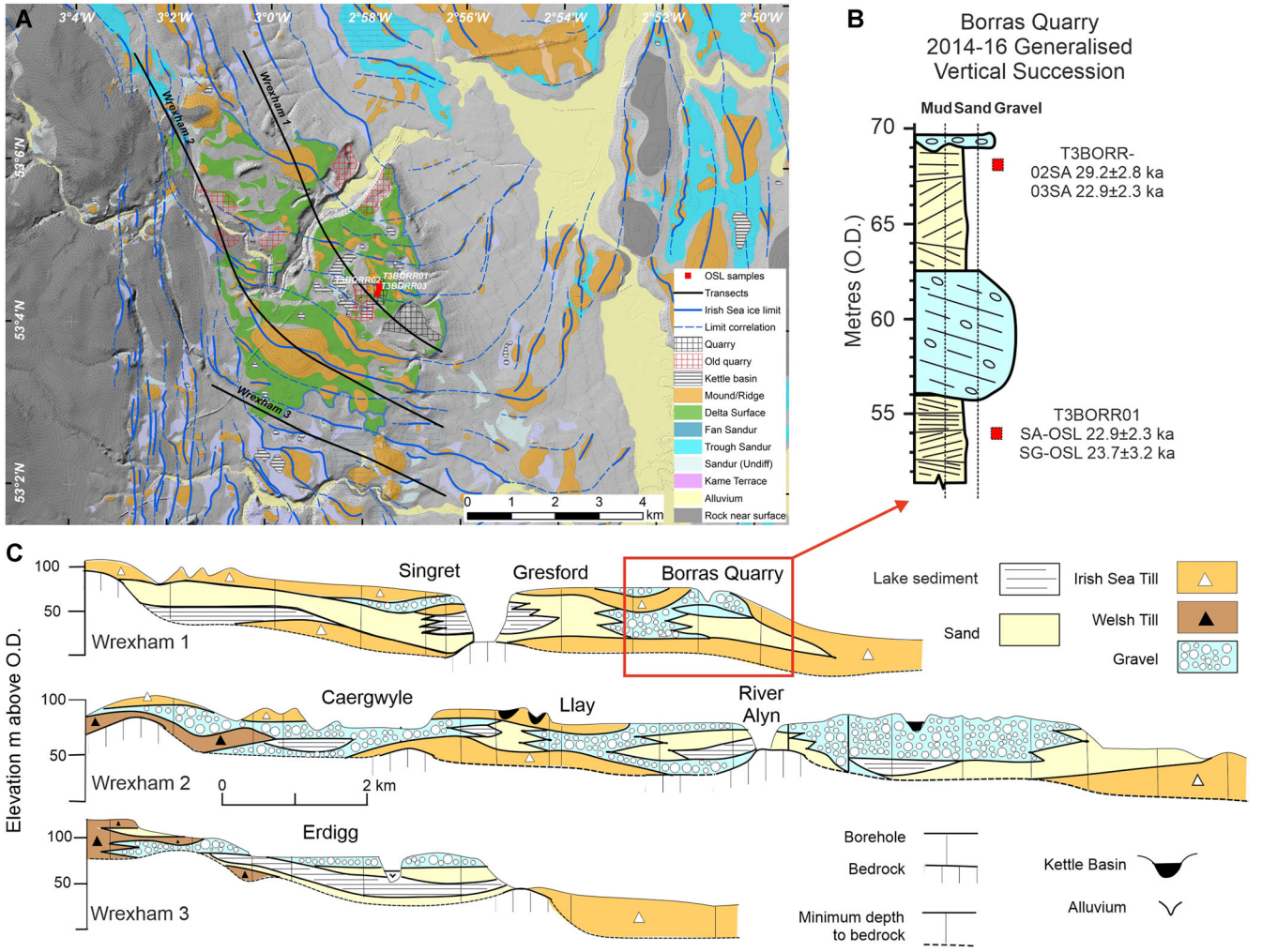

Figure 10. (A) Glacial geomorphology of the Wrexham delta around Borras Quarry. (B) Generalized vertical succession of the 2013–2017 exposures at Borras, the locations and ages obtained for samples T3BORR01-03. (C) Borehole cross-sections extending across the Wrexham delta towards Glacial Lake Bangor. The cross-section lines are shown in A. [Color figure can be viewed at wileyonlinelibrary.com]

and T3WOOD05 overlap within uncertainties and date the Oswestry–Whitchurch–Congleton (L4) configuration of the ice margin (Fig. 1C) and the abandonment of Glacial Lake Prees (Figs 6 and 9).

Zone 6: Glacial Lakes Bangor and Delamere in lowland Cheshire

Running parallel to the western margin of the ISG were a series of NE–SW orientated moraines that confine the Mold –Caergwyle ice-marginal sandur (Thomas, 1985a, 1989, 2005); this was the main outwash feeder for the >50-km^2 Wrexham delta (Fig. 10A) (Thomas, 2005). The eastern frontal slopes to the delta terrace are raised <30 m overlooking the Dee Valley, and since first description (Wedd *et al.*, 1927) the terrace has been identified variably as a delta, alluvial fan and outwash sandur (Peake, 1961, 1979, 1981; Poole and Whiteman, 1961; Wilson *et al.*, 1982; Worsley, 1985). Comprehensive morphological and sedimentological analysis (Thomas, 1985a, 1989, 2005) has revealed areas of ice-disintegration terrain (melt-out basin or pitted sandur), ice front fan, ice-marginal sandur, and a proglacial to ice-contact delta, all of which fed into a large former lake basin called Glacial Lake Bangor (Fig. 10) (Thomas, 1985a, 1989). The serial sections have been devised from exposures and borehole data (Fig. 10A,C). For the delta to function ice is required to be in contact with both the Mold –Caergwyle ice-marginal sandur and the delta slopes immediately to the north of the terrace. Borras Quarry has provided access to exposures towards the distal end of the Wrexham delta (Fig. 10C). A composite >15-m vertical succession was developed in 2014–2016 using a series of quarry faces that were limited in height to 2–3 m (Fig. 10B). T3BORR01 sampled horizontally stratified medium to coarse sands deep within the sequence that appear to be low-angle delta fore-sets given adjacent units of trough cross-stratified gravel, granule and sand. Within 2–4 m of the delta surface (~70 m O.D.), T3BORR02 sampled horizontally stratified fine to medium sands and T3BORR03 rippled fine to medium sands, both of which were from delta top-set outwash deposits that showed a planar geometry. All three SA-OSL D_e distributions were asymmetrical and were therefore probably heterogeneously bleached before deposition (Fig. 2F). T3BORR01 underwent parallel SA-OSL and SG-OSL analyses returning similar minimum D_e populations and ages. OSL ages of 22.9 ± 2.3, 23.7 ± 3.2 and 22.9 ± 2.3 ka are tightly clustered, whereas sample T3BORR02 appears older at 29.2 ± 2.8 ka, indicating that this SA-OSL age is an overestimate including D_e values potentially from partially bleached grains.

Discharge from the ISG margin between the ice and the mid-Cheshire sandstone ridge has formed an extensive wedge-shaped terrace of ice-contact kame and pitted outwash delta surfaces. This flat terrace extends 10 km as a wedge southward and has a pitted surface with kettlehole basins (e.g. Hatchmere). Bordered in the east by a probable ice-contact slope, the feature resembles the Wrexham delta (Thomas, 1985a) in its morphology (Fig. 1C). Sediments exposed in the former

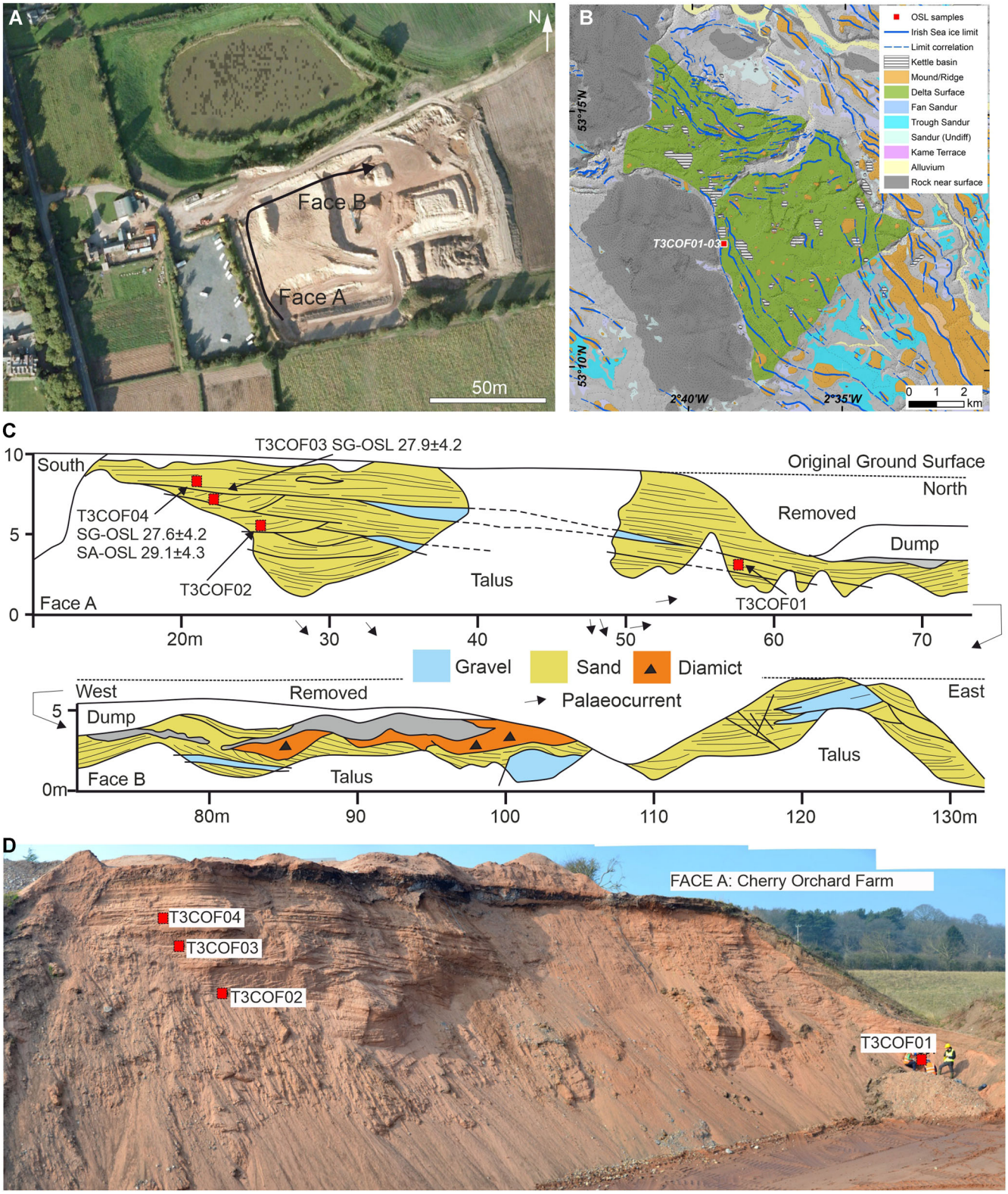

Figure 11. (A) Quarry aerial photograph and quarry plan at Cherry Orchard Farm as visited in 2014. (B) Glacial geomorphology and postglacial sediments of the Delamere delta around Cherry Orchard Farm Quarry (T3COF01-03). (C) Serial lithological succession of the 2013 exposures at Cherry Orchard Farm. (D) Photomontage of Quarry Face A at Cherry Orchard Farm. C and D also include the locations and ages obtained for samples T3COF01-04. [Color figure can be viewed at wileyonlinelibrary.com]

Cherry Orchard Farm Quarry (Fig. 11A) have been OSL dated to constrain an ice-marginal configuration straddling the terrace (Fig. 11). The 2013 exposures showed a 10-m-thick sequence of predominantly sand with occasional sand and gravel overlying at depth a diamicton (Fig. 11C). The upper 8 m was dominated by low-angle trough and planar cross-beds of stratified medium–coarse sand with granule to pebble gravels dipping south-east interpreted as delta fore-set beds and deposited as cohesionless debris-flows into a < 20–30-m deep proglacial lake (Smith and Ashley, 1985; Nemec *et al.*, 1999; Nemec, 2009). The cross-cutting nature of the cross-sets probably reflects scour and variations in flow direction on the low-angle delta front (Fig. 11C). The depositional environments graded from delta-proximal

toe-set or bottom-sets sands, through stacked units of trough cross-stratified granular sands laid down as cohesionless debris flows in subaqueous channels on the delta front. The units contain occasional out-sized clasts that are probably dropstones. T3COF03 sampled one of the uppermost trough cross-stratified channel fills, whereas T3COF04 sampled horizontally stratified sands probably laid down in relatively shallow water on a low-angle delta fore-set slope near the top of the sequence (Fig. 11D). The three D_e distributions (Fig. 2E) determined for samples from Cherry Orchard farm were asymmetrical and therefore heterogeneously bleached before burial. The D_e distributions characterize the minimum dose population well and so the OSL ages appear to reflect the true burial age. The SG-OSL ages of 27.9 ± 4.2 ka (T4COF3) and 27.6 ± 4.2 ka (T4COF4) and SA-OSL age of 29.1 ± 4.3 ka (T4COF4) date the L6 configuration of the ice margin and timing of Glacial Lake Delamere (Fig. 11B).

Zones 8 and 9: deglaciation of lowland Lancashire

Retreat of the ISG margins northwards (Fig. 1B) into Lancashire led to an increasing influence of differing ice sources (Irish Sea, Cumbria and Ribble Valley) over the configuration of the ice-marginal geomorphology (Fig. 12A). Exposure of the stratigraphy in the region has been scarce since the coastal revetment of the former cliff sections at Blackpool (De Rance, 1877), and limited to Lydiate Lane and Bradley's Quarries (Fig. 12A) providing the only substantial glacigenic exposure as described by Chiverrell *et al.* (2016). Retreat of Cumbrian ice margins north of the Ribble and the RVG margins eastwards while the ISG was still in a more advanced position led to the establishment of an ice-dammed proglacial lake, with the large debris fan west of Lydiate Lane Quarry (Fig. 12A) formed by flows into that lake basin. The Kirkham Moraine (BL6) is a substantial moraine complex that extends ~30 km E–W across central Lancashire (Fig. 1) (Gresswell, 1967; Chiverrell *et al.*, 2016). Lydiate Lane exploits a bench interpreted as an ice-contact kame terrace, ice limit L8 (Fig. 1B), between the eastern margin of Cumbrian ice and the West Pennines Moors, and comprises a thick sequence of outwash sands and gravels (Chiverrell *et al.*, 2016). Further north, exposures at Bradley's Quarry exploit an E–W aligned trough sandur, bounded by moraine ridges to the north and south (Fig. 12A). The ridges of the Kirkham Moraine trend west before curving north-west towards the coast and form ice limit L9 (Fig. 1B). The ridges are separated by sandur flats and punctuated by numerous kettle basins showing a significant presence of former dead-ice within the moraine complex.

Lydiate Lane Quarry has evolved rapidly from March 2013 to the present (Fig. 12B), and the working faces have revealed a generalized vertical succession of <15 m of outwash sands and gravels overlying a > 2-m basal diamicton (see Chiverrell *et al.*, 2016). The reddish sand and gravels reflect their derivation from eroded Permo-Triassic sandstones and contain numerous Cumbrian erratic clasts (e.g. Shap granite). The deposits reflect an evolution from an ice-proximal to more distal sandur lithofacies (Thomas *et al.*, 1985), with the upper of these cycles produced by prograding bar-forms and channel migration (Miall, 1977; Thomas *et al.*, 1985). T3LYDL04-6 (Fig. 12C,D) were taken from rippled medium to coarse sand (Sr) between thin units of planar cross-set coarse sand (Sp), with all three samples lain down in relatively low-energy settings, in theory with reasonable opportunities for bleaching. However, the SA-OSL D_e distributions for T3LYDL04-05 and SG-OSL distributions for T3LYDL06 suggest that the samples were heterogeneously bleached (Fig. 2G). The SA-OSL ages of 30.9 ± 5.2 ka (T3LYDL04) and 44.5 ± 3.9 ka (T3LYDL05) and the SG-OSL age of 57.2 ± 13.1 ka (T3LYDL05) in theory constrain the L8 configuration of the ice margin (Fig. 1B). A clearer picture emerges from analysis of two cobbles at Lydiate Lane that yielded ages of 30.2 ± 1.1 ka (T3LL1D-04) and 30.3 ± 1.4 ka (T3LL1D-09). The pattern of age with depth into these cobbles, especially T3LL1D-09 that has seven slices to a depth of 5.0 mm that give consistent ages (Fig. 3c), is strong evidence that the last exposure to daylight for these samples was at that time. However, these ages pre-date the timing of advance to maximum limits at Bridgwalton, which if taken at face value suggest the deposits at Lydiate Lane relate to an earlier glacial episode, with the cluster of ages around 30 ka constraining the advance of the ice sheet during the build up towards the LGM. The setting at Lydiate Lane is intriguing, with the deposits forming a lateral bench or series of benches at 50–80 m O.D. wedged against the 200–300-m bedrock rise to the West Pennines Moors. The deposits display no evidence for over-consolidation and structural deformation that might be expected had there been later over-ride by ice, particularly so given the numerous ice-marginal ridges in the immediate vicinity (Fig. 12A). An alternative explanation is that the Lydiate Lane deposits are younger and relate to the most recent deglaciation, but the OSL signals for these samples had not been reset. The quantity of analysis undertaken here is substantial, assessing >17 000 grains and two cobbles; perhaps the transport distances from the ice margin were very short and the kame environment may have been a turbid subaqueous shallow lacustrine setting rather than outwash sandur. The chronology and context derived at Lydiate Lane remains equivocal.

The sections at Bradley's Quarry have also evolved with time (Fig. 13A) and description of the exposures from 2009–2016 has shown >25 m vertical succession (Fig. 13B) (see Chiverrell *et al.*, 2016), with the upper units of distal outwash deposits (Thomas *et al.*, 1985; Sambrook Smith *et al.*, 2005, 2006) sampled for OSL dating. Samples T3BRAD03-05 (Fig. 13C,D) were taken from adjacent rippled medium to coarse sands (Sr) from relatively low-energy flows with reasonable opportunities for bleaching in this upper and distal sandur succession (Thomas *et al.*, 1985). SA-OSL (T3BRAD04-05) and SG-OSL (T3BRAD06) D_e distributions suggest that all samples were heterogeneously bleached (Fig. 2H), but they contain a minimum dose population that may reflect the burial age. The SA-OSL ages were 28.7 ± 2.5 ka (T3BRAD03) and 25.2 ± 2.3 ka (T3BRAD04), and the SG-OSL age was 45.7 ± 5.2 ka (T3BRAD06). The SA-OSL ages appear a little old and the SG-OSL age substantially too old in constraining the timing of this ice margin configuration (L9: Fig. 1). The rationale for poor resetting of the OSL signal is less clear at Bradley's Sandpit given the low-energy sandur environment and again the quantity of analysis was substantial, assessing >20 000 grains.

Bayesian age modelling of the deglaciation

Bayesian age modelling (Bronk Ramsey, 2009a) of the dating control calculates the timing for the advance and retreat northwards of the ISG across the Shropshire, Staffordshire, Cheshire and Lancashire lowlands. Ultimately, Bayesian analysis produced a conformable age model (Fig. 14; Table 3) with an overall agreement index of 109%, thus exceeding the >60% threshold advocated by Bronk Ramsey (2009a). Italics denote the posterior density estimates or modelled ages derived from the Bayesian modelling throughout to distinguish them from the unmodelled individual ages of directly dated samples. Pre-dating ice advance to LGM limits were radiocarbon ages from Four Ashes (Morgan, 1973) and the OSL ages

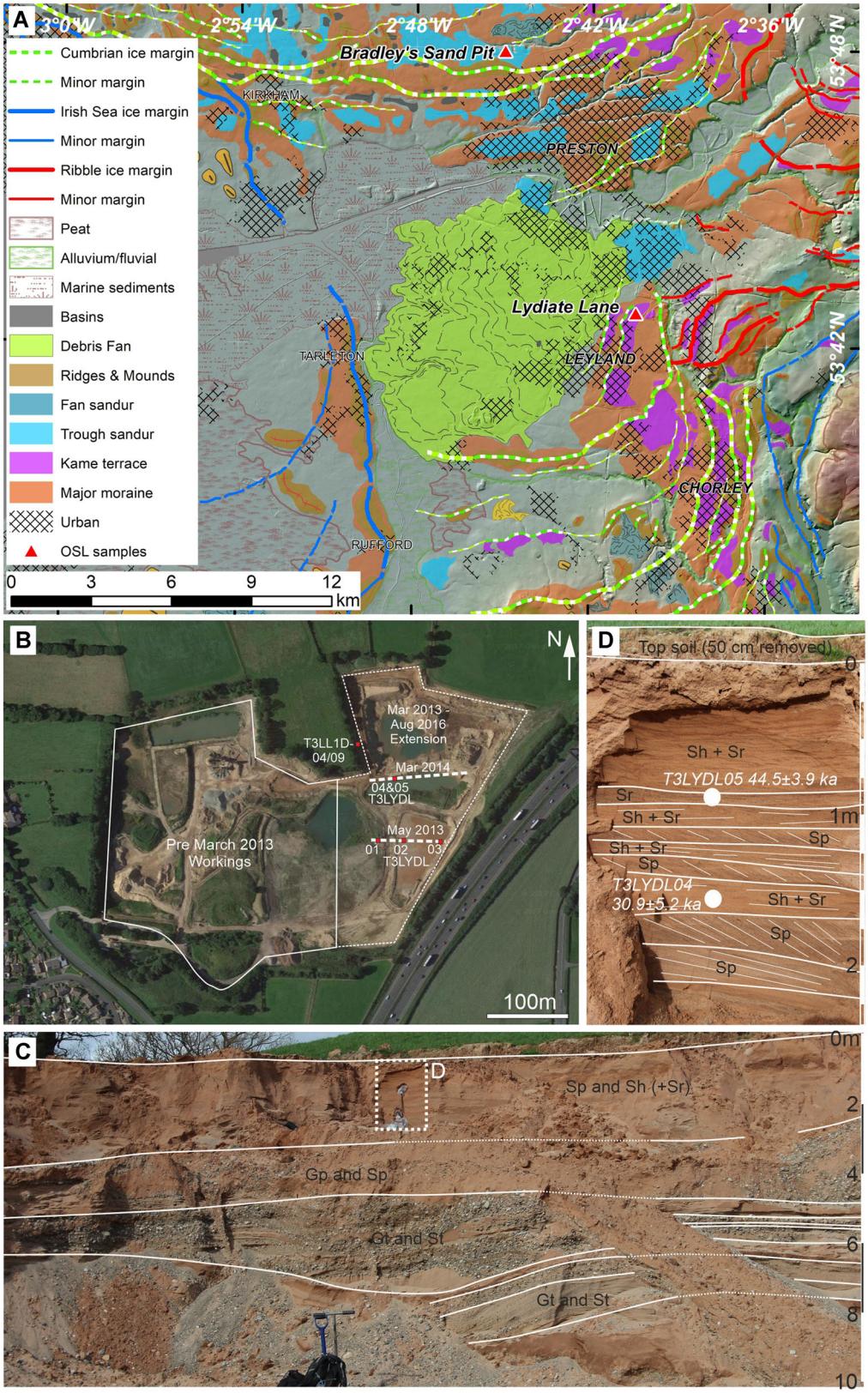

Figure 12. (A) Glacial geomorphology and postglacial deposits of central Lancashire identifying the location of OSL sites at Lydiate Lane and Bradley's Quarries (Fig. 13). (B) Aerial photograph image (© Getmapping PLC Aerial EDINA Digimap) of the evolution of the Lydiate Lane Quarry, overlain by the pit outlines investigated in 2013–2016, as well as the section faces sampled for OSL dating. (C) Annotated photographs of the stratigraphy yielding samples T3LYDL04-05 and the extent of part D (white pecked). (D) Close up of the stratigraphy showing the locations and ages obtained for OSL samples T3LYDL04-05. Lithofacies code annotations denote sand units with Sh horizontal stratification, trough (St) and planar (Sp) cross bedding and rippled sands (Sr). Gravel units comprise trough (Gt) and planar (Gp) cross bedding. [Color figure can be viewed at wileyonlinelibrary.com]

from Dowkabottom (Telfer *et al.*, 2009), and these were supported here by the cluster of OSL ages around 29.9 ± 1.2 ka from Lydiate Lane Quarry in constraining the advance of ice into the region. In Zone 1, six OSL ages from Bridgwalton and Seisdon produced good agreement with the model, but the SG-OSL ages for T3SEIS01 and T3SEIS02 were treated as outliers. Thus, ice advance to maximum limits occurred after *28.2 ± 1.4 ka* and before *25.5 ± 1.2 ka*, with an ice margin

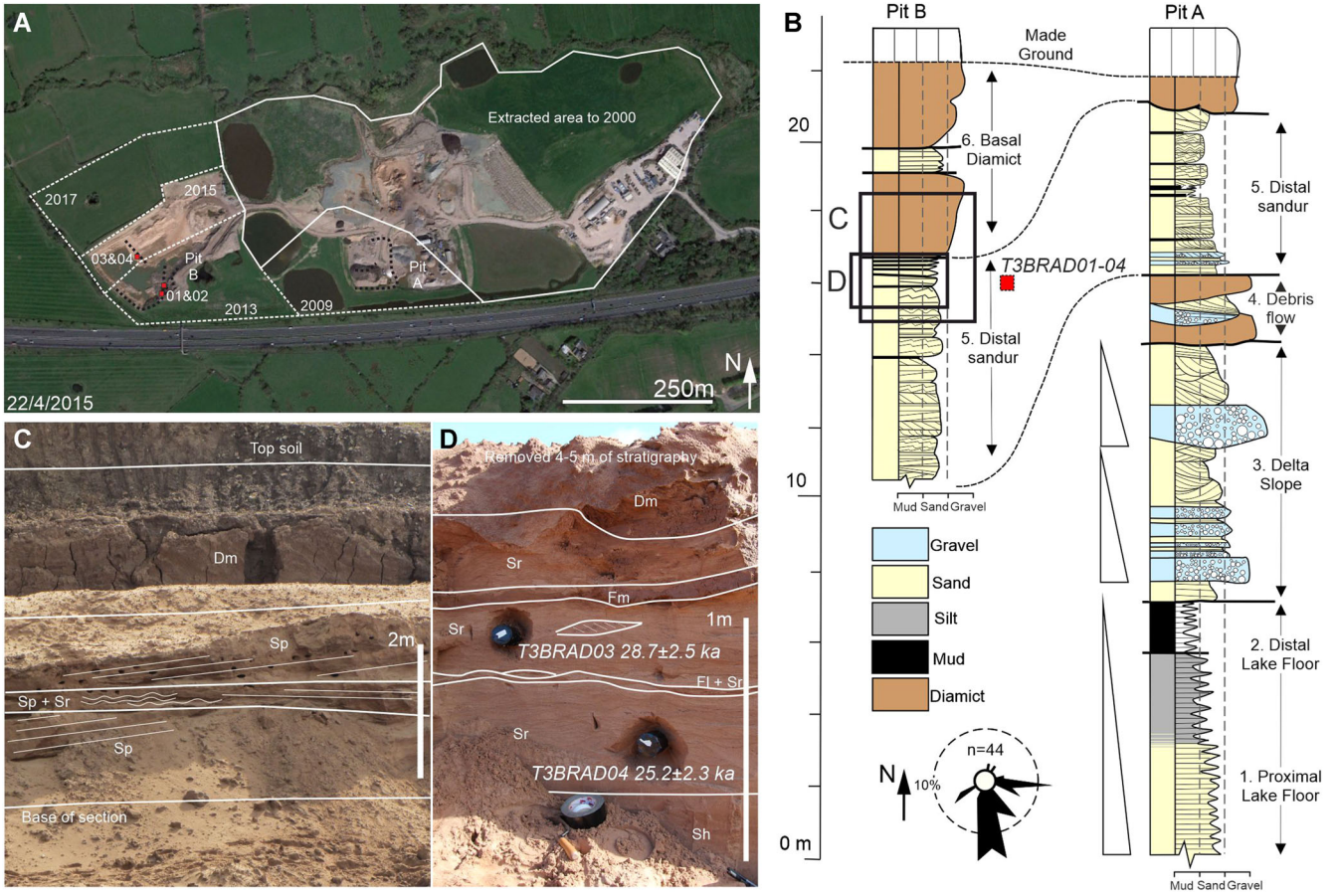

Figure 13. (A) Aerial photograph (© Getmapping PLC Aerial EDINA Digimap) showing the development of Bradleys Sandpit (Fig. 1B), overlain by the pits as investigated in 2009, 2013 and 2017, as well as the main section faces (dotted black lines) and locations sampled for OSL dating T3BRAD01-04 (red dots). (B) A summary of generalized vertical successions (GVS) of the exposed sequences, including a rose diagram of palaeocurrents measured for the sequence. (C–D) Annotated photographs of the stratigraphy in Pit B, showing the locations and ages obtained for OSL samples T3BRAD03-04, with lithofacies code annotation denoting: Dm – massive diamict, Sp – planar cross-stratified sands, Sr – rippled sands and Fm – massive fines. The stratigraphical position of the photographs is shown on the Pit B GVS. [Color figure can be viewed at wileyonlinelibrary.com]

discharging into Glacial Lake Morville *26.5 ± 1.1 ka*. The inner shoreline of Glacial Lake Newport (Zone 2) was more challenging to date, with three ages being clear outliers (T3COND03-SG and –SA, T3COND05), but T2COND02 gives a better but low (42.5%) agreement with the age range refining to *25.5 ± 1.2 ka*. However, given the potential for readvance of Welsh ice influencing the site, the original age of 19.7 ± 2.5 ka for T3COND02 is regarded as a better fit. Given that the Welsh ice advance was in part contemporary with the ISG ice margins at or near to the Wood Lane site, T3COND02 arguably would be better positioned in the Bayesian sequence model as part of the Phase Zone 5 (Fig. 14). The Oswestry–Whitchurch–Congleton moraine OSL ages produce a good agreement in the model, with T3WOOD05 a minor outlier (48%) and slightly too young (Fig. 14). Ice margin retreat to the L4 limits occurred after *24.3 ± 1.1 ka*, with an ice margin discharging into sandur around Wood Lane *23.9 ± 1.0 ka*. Two sites, Borras and Cherry Orchard Farm Quarries, constrain the dynamics of proglacial lakes and ice margins in the Dee and Weaver basins. Dating the materials at Cherry Orchard Farm was challenging, but the OSL ages overlap within uncertainties; they are conformable within the model producing an average modelled age of *23.3 ± 1.0 ka* which is towards the young end of the measured 2σ uncertainties. The OSL ages from Borras, with the exception of the complete outlier T3BORR02-SA, form a tight cluster centred on a modelled age of *22.5 ± 1.0 ka*. Together these sites constrain the retreat of ice margins into Glacial Lakes Bangor and Delamere to after *23.6 ± 1.0 ka* (L4), with ice margin retreat northwards into Lancashire by *22.1 ± 1.0 ka* (L5 to L6). The chronology for ice margins in Zones 8–9 was challenging, with only one out of eight ages producing a weak agreement with this phase in the age model. The Lydiate Lane chronology is a better fit and has been included earlier in the model documenting the advance stage build up to the LGM advance. The OSL measurement for T3BRAD04-SA is a minor outlier (52.8%) and has produced a modelled age of *21.5 ± 1.1 ka*, but much of the constraint on this comes from well-dated sites further south and ages from further north documenting the retreat of ice margins into north Lancashire, the Isle of Man and SW Cumbria by *20.5 ± 1.3 ka* (L9: Fig. 14), and then ultimately into upland Cumbria and the Pennines by *17.5 ± 0.8 ka* (L10: Fig. 14). In summary, the Bayesian modelling has calculated modelled age probability distributions for ice limits of *28.2 ± 1.3 to 25.4 ± 1.2 ka* (L1), *23.6 ± 1.0 ka* (L4), *22.1 ± 1.0 ka* (L5 to L6) and *20.5 ± 1.3 ka* (L9).

Discussion

Influence of lake-terminating ice margins

The Irish Sea sector was unusual in the former BIIS in feeding ice towards two disparate termini: in the east the lake/land-terminating ISG and in the west the marine-terminating ISIS. Terrain in the lowlands of northwest England and Midlands lacks convincing evidence for higher ice velocities in the form of elongated bed forms unlike the ISIS to the west

(Van Landeghem *et al.*, 2009). It also terminated on land at maximum limits extending into the English Midlands (Fig. 1). Extensive proglacial lakes formed during the LGM advance and retreat stages between the ISG and the reverse bedrock slopes (Fig. 15) that generally fronted these former ice margins (Wills and Dixon, 1924; Wills, 1948; Shaw, 1972a, 1972b; Worsley, 1975, 2005; Thomas, 1989, 2005). This complex bedrock topography provided numerous niche opportunities for establishing localized ice-marginal lakes (Wills and Dixon, 1924). The lake extents presented here are not compatible with the more extensive definitions of 'Lake Lapworth' (see discussions in Maw, 1864; Watts, 1898; Harmer, 1907; Wills and Dixon, 1924; Poole and Whiteman, 1961; Worsley, 1975; Thomas, 1989; Murton and Murton, 2012), but show instead a time transgressive sequence of smaller lakes that developed and evolved with retreat of the ice margins (Thomas, 1989). The geochronology presented here is the first time that dating of the evolution of these lakes has been attempted. The styles of lake vary from bedrock-confined ice contact lakes (e.g. Glacial Lake Morville; Fig. 7), ubiquitous ice disintegration hollows and kettle basins concentrated in the Oswestry–Whitchurch–Congleton moraine complex (Fig. 6), to proglacial lakes confined by the fronting topography (e.g. Glacial Lake Bangor; Fig. 10).

Downstream of Ironbridge Gorge (Zone 1), slopes normal to the ice flow direction drained south and limited glacial lakes to localized ponding between the ice margins and bedrock terrain (e.g. Glacial Lake Morville and others as described by Wills and Dixon, 1924). North of the Wenlock Edge – Wrekin escarpment (Zone 1/2 boundary), slopes reverse to the ice flow direction ponded initially small and latterly more substantial compound lakes. Glacial Lakes Newport/Buildwas expanded and combined with the north-westerly retreating ice margin. The lake spillways drained east feeding the River Trent (Gnosall) and increasingly south to the River Severn with (re-)incision at Ironbridge Gorge. Continued ice margin retreat led to the development of proglacial lakes north of the moraine and bedrock highs at limits L4 (Glacial Lake Prees)

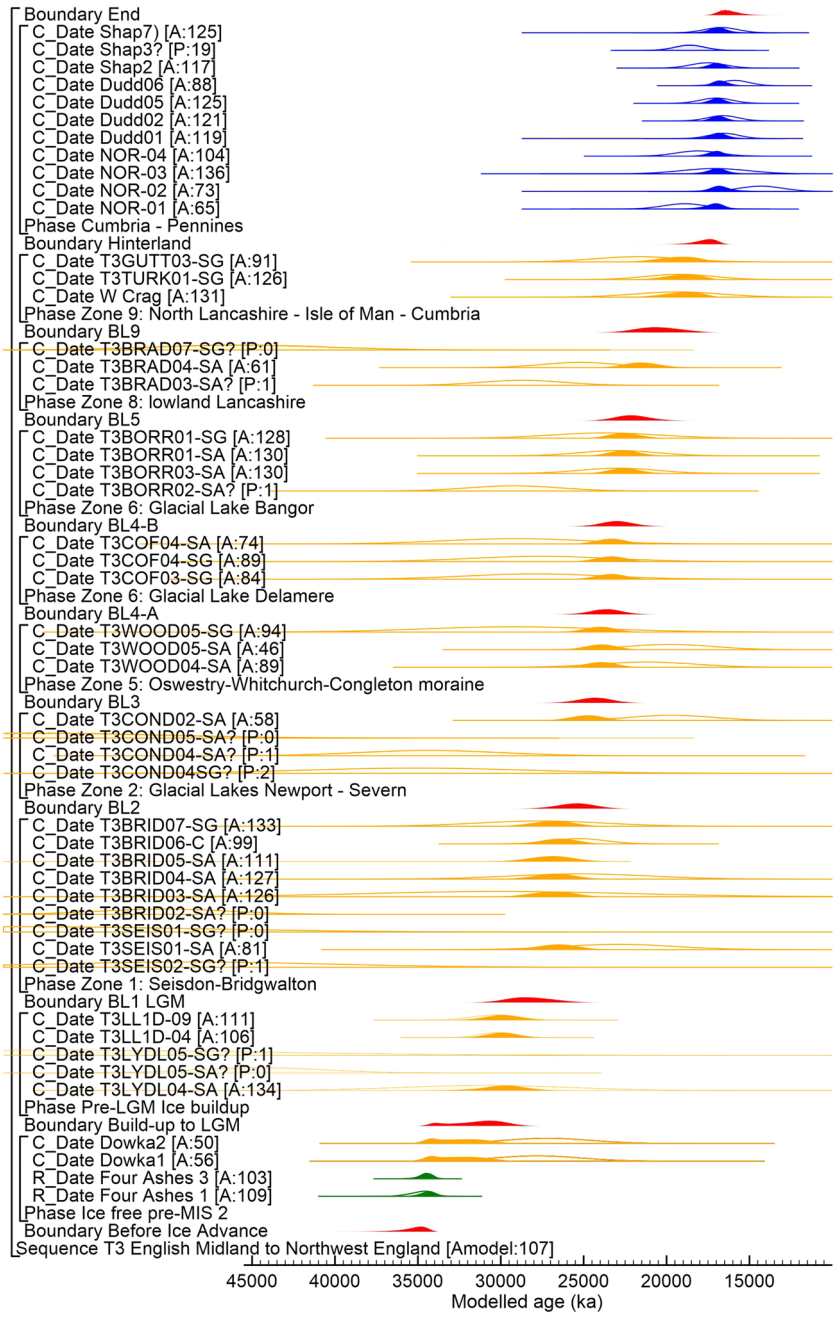

Figure 14 Bayesian model for the dating of ice retreat across from the English Midlands into the northern Irish Sea basin. Geochronology includes the ages presented here, alongside published ^{14}C ages from Four Ashes (Morgan, 1973), OSL ages from Dowkabottom and Warton Crag (Telfer *et al.*, 2009), Four Ashes (Morgan, 1973), OSL ages from the Isle of Man (T3TURK01) and SW Cumbria (T3GUTT03) (Chiverrell *et al.*, 2018), and cosmogenic nuclide ages from Shap, the Duddon Valley and Norber (Wilson *et al.*, 2012b, 2013, 2018). The model structure shown uses OxCal brackets (left) and keywords that define the relative order of events (Bronk Ramsey, 2009a). Each original distribution (hollow) represents the relative probability of each age estimate with posterior density estimate (solid) generated by the modelling. Shown are ^{14}C ages (black), OSL ages (orange), cosmogenic nuclide ages (blue) and modelled boundary ages (Red). Outliers are denoted by '?' and their probably (P) of being an outlier indicated by low values <5 (95% confidence). Model agreement indices for individual ages show their fit to the model with >60% the widely used threshold for 'good' fit (Bronk Ramsey, 2009b). [Color figure can be viewed at wileyonlinelibrary.com]

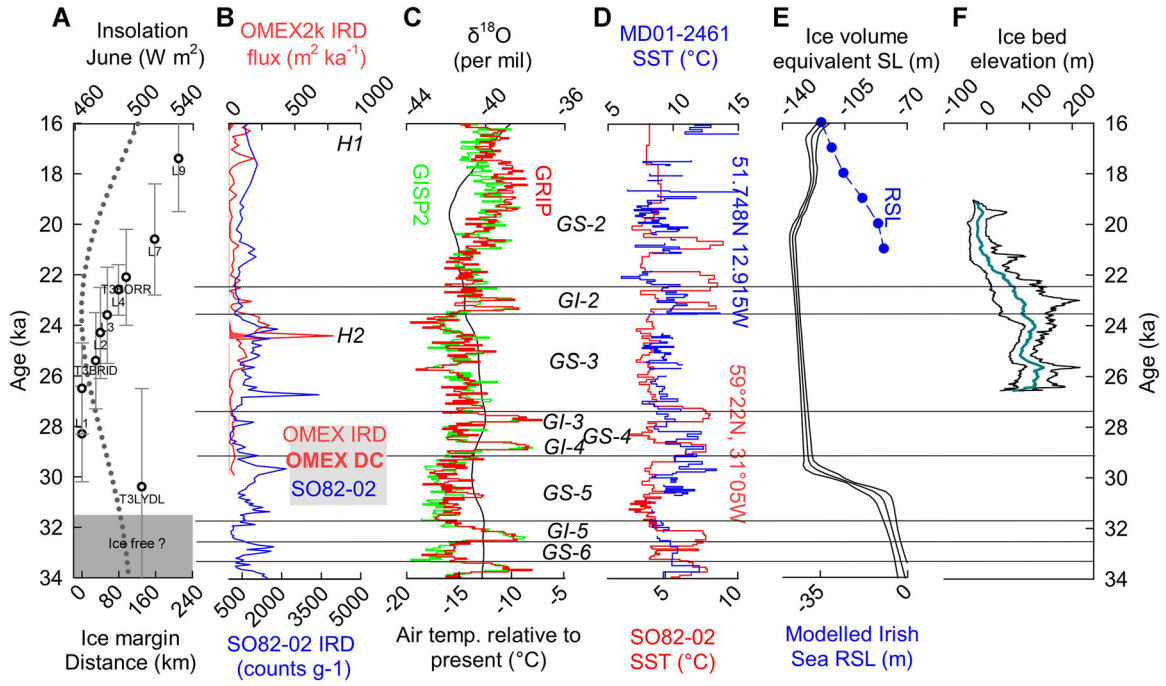

Figure 15. (A) The boundary ages (circle ± 1 sigma whisker plots) from the Bayesian model plotted against net axial retreat distance and summer insolation (pecked) for 60°N (Berger and Loutre, 1991). (B) The dolomitic carbon (DC – solid orange) and total ice-rafted debris (IRD – grey outline) flux records from the OMEX2K marine core from the Goban Spur continental slope SW of Ireland (Haapaniemi *et al.*, 2010) and the North Atlantic core SO82-2 from the Reykjanes Ridge at 59°N (Moros *et al.*, 2002; Rasmussen *et al.*, 2016; Waelbroeck *et al.*, 2019). Heinrich Events H2 and H1 are highlighted (Bond *et al.*, 1992). (C) $\delta^{18}O$ concentrations, Greenland Stadials (GS) and Interstadials (GI) from the GISP2 and GRIP Greenland ice cores (Rasmussen *et al.*, 2014). (D) Sea surface temperature records determined for the North Atlantic using SST (°C) calculated using planktonic foraminifera for core SO82-02 at 59°N, 31°W (red line) (Van Kreveld *et al.*, 2000; Rasmussen *et al.*, 2016) plotted using an updated age model (Waelbroeck *et al.*, 2019) and the MD01-2461 site from the Porcupine Seabight at 51.7°N, 12.9°W (blue line) (Peck *et al.*, 2006, 2007). (E) Ice volume equivalent sea level (Lambeck *et al.*, 2014) and modelled relative sea level for Anglesey (blue dots) derived from a glacial isostatic adjustment [GI(A) model (Bradley *et al.*, 2011)]. (F) Mean and 95% trough elevations estimated from the NEXTMap elevation and EMODnet bathymetry (http://www.emodnet-hydrography.eu/) datasets plotted against the modelled boundary ages (Fig. 14). [Color figure can be viewed at wileyonlinelibrary.com]

and L5 (Glacial Lakes Bangor and Delamere) (Wills and Dixon, 1924; Wills, 1948; Thomas, 1985a, 1989). Glacial Lake Severn (Fig. 5) is unusual in that it takes the form of an over-deepening >150 m extending below present sea level, probably excavated under ice compression against the Wenlock Edge bedrock rise to the east (near Shrewsbury) but also potentially compressional stresses driven by ice collision where Welsh ice met the ISG. This degree of over-deepening may be unique in lowland England outside of the mountain regions (e.g. Windermere, English Lake District). Exposures of glacilacustrine deposits are rare, although former exposures at Buildwas showed evidence for materials (e.g. diamict rafts) released from floating ice (Wills and Dixon, 1924), which point to calving ice margins associated in part with the evolution of these lakes. The widespread presence of glacilacustrine environments fronting the retreating ISG margins potentially regulated the dynamics and nature of the marginal retreat. Mechanical calving, surface melt and subaqueous melt all control ablation at subaqueous ice margins (King *et al.*, 2018). Given the probable low salinity, low temperatures and limited water circulation typical of these types of lake, enhanced subaqueous melt is an unlikely factor, but increasing water depths towards full ice thickness would initiate more rapid mechanical calving and as a consequence marginal retreat (Kirkbride, 1993, 1995; Brazier *et al.*, 1998; King *et al.*, 2018). Retreat of ice from the English Midlands would potentially have been punctuated by episodes of slower land-terminating retreat, marginal instability and then accelerated retreat with the transition to a glacilacustrine calving ice margin, then slowing as prograding deltas and passage of ice margins onto land isolated the ice front from these lake basins.

Advances in geochronological methods

This study is the first to apply a combination of SA-OSL, SG-OSL and cobble-based OSL methods to date glacial sediments. The distributions of D_e values obtained for all the sediment samples (SA-OSL and SG-OSL) are more scattered than can be explained by the measured uncertainties on individual aliquots, and this scatter is likely to result from incomplete resetting of the OSL signal in some grains at the time of deposition. Unlike some other studies of glacial sediments of similar age, no samples are seen in this study where all grains have had their OSL reset at deposition (cf. sites in the Isles of Scilly; Smedley *et al.*, 2017b). In this study, models designed to extract the lowest dose population have been used to calculate the D_e for use in age calculation in Table 2. The proportion of the grains in any given sample that were exposed to enough daylight at deposition to reset the OSL signal will vary, for example T3BRID07 and T3WOOD05 provide an interesting contrast. T3BRID07 (Fig. 2A) has a clear population of grains with a D_e of ~38 Gy that is picked out by the MAM, and these are apparent in the kernel density estimate as a distinct peak. A range of grains with higher D_e values are also seen, with values appearing to cluster between 150 and 250 Gy, but these are likely to be close to saturation. A clear differentiation of grains in this way was seen in similar samples from glacial sediments in eastern Ireland (Small *et al.*, 2018, figure R3). In contrast, T3WOOD05 appears to have a very small proportion of grains that had their signal reset, whether measured on small aliquots or on single grains (Fig. 2D). This latter type of sample is common in this transect, and OSL dating of such samples, whether using single grains or small aliquots, is challenging. It is also plausible that some of the samples either have no grains

that had their OSL signal completely reset at the most recent cycle of erosion and deposition, or that the proportion of grains that were reset was so small that it has not been possible to identify them using the statistical approaches used here. A critical part of the analysis has been to collect multiple samples from sites, use multiple scales of analysis, use cobbles for dating at selected sites and use a Bayesian framework to identify outliers.

SA-OSL and SG-OSL ages are within errors for the deposits at Cherry Orchard Farm, Wood Lane and Borras Quarries. While no direct comparisons were made at Bridgwalton, the SG-OSL and cobble ages are similar, as are two of four of the SA-OSL ages. The SA-OSL and SG-OSL measurements do not agree at Seisdon, but these were particularly poorly bleached sediments. On this basis we believe that our methodologies are consistently extracting the most bleached component of the D_e distribution. However, given the complexity of the D_e distributions and the very small component of many of the samples that appear to have been bleached, the extracted final D_e used for age calculation purposes may still include some poorly bleached grains leading to age over-estimation. Given the ice-marginal contexts sampled, the sedimentation rates may have been very high, the sediment transport pathways short and water columns opaque with heavy sediment loads. As a result, it is not a surprise that sunlight exposure was often insufficient to bleach samples before burial. Bayesian analysis of sites and samples within zones supports this by identifying outlier ages which were affected particularly by poor bleaching. Age over-estimation is less of an issue for the cobble approach because poorly bleached cobbles were identified and not analysed. This, along with a lower reliance on understanding palaeo-moisture fluctuations, has led to a lower uncertainty for the cobble ages.

Forcing of the glacial dynamics

The build-up and advance of the BIIS into NW England had not been dated previously (Chiverrell and Thomas, 2010; Hughes *et al.*, 2016a). Ice-free conditions are evidenced in the central Scottish sector of the ice-sheet and radiocarbon dated to 33.1–34.4 ka BP at Sourlie (40 km SW from Glasgow, 55°38′ 18.80″N, 4°38′31.46″W) (Jardine *et al.*, 1988; Bos *et al.*, 2004) and 31.5–34.8 ka BP at Balglass Burn (20 km north of Glasgow, 56°02′N, 04°17′W) (Brown *et al.*, 2007). Those radiocarbon ages are similar to the 35–34 cal ka BP range obtained for equivalent ice-free conditions at Four Ashes in the English Midlands (Morgan, 1973). Here, we use the convergence of quartz grain- and granite cobble-based OSL ages from Lydiate Lane to show that by 30.2 ± 1.1 and 30.3 ± 1.4 ka eastern Lake District and Irish Sea (Galloway Hills) ice masses had advanced 65 and ~150 km, respectively, into south Lancashire. The Lydiate Lane kame complex requires an ice margin abutting against the lower slopes (50–90 m O.D.) of the West Pennines (maximum elevation 450 m). The Lydiate Lane deposits contain ISB and Lake District erratic cobbles including Shap granite and volcaniclastic sediments (Borrowdale Volcanic Group). The lack of deformation in the sequence (e.g. consolidation, faulting or folding) point to limited subsequent override by ice on this eastern margin. Later expansions of Irish Sea ice to LGM limits *28.3 ± 1.9–26.5 ± 1.8 ka* in the English Midlands and ~26 ± 1.5 ka in the south Celtic Sea (Praeg *et al.*, 2015; Smedley *et al.*, 2017b; Scourse *et al.*, 2019), coupled with faster ice flows down the axis of the Irish Sea (Van Landeghem *et al.*, 2009), may have reduced ice flows towards this less dynamic eastern ice margin. Our discussion of ice margin advance and retreat rates reflects the net movement of ice margins and by necessity integrates smaller episodes of margin advance, slowdown, stillstand, retreat and acceleration. Build-up of ice, from what were probably reduced-ice or ice-free conditions in Britain 34.8–31.5 ka (Fig. 15A), comprised net marginal advance rates of 100–46 m a^{-1} from the uplands of SW Scotland and NW England into south Lancashire by 30.3 ± 1.4 ka.

The subsequent LGM advance of the ISG occurred from *28.3 ± 1.9 ka* (Fig. 15A), reaching and ponding Glacial Lake Morville at the maximum limit at *26.5 ± 1.8 ka*. This ice margin advance of 130 km occurred at ~50 m a^{-1}, and was coeval with the shift to colder conditions of Greenland Stadial 3 (GS-3) (Fig. 15C), a colder North Atlantic (Fig. 15D) and the June insolation minimum (Fig. 15A) (Berger and Loutre, 1991; Van Kreveld *et al.*, 2000; Peck *et al.*, 2007; Rasmussen *et al.*, 2014, 2016). The chronology for the ISG maximum is equivalent to dating of maximum limits to the west for the ISIS on the Isles of Scilly at 26 ± 1.5 ka (Smedley *et al.*, 2017b) and in the south Celtic Sea at 27–24 ka (Praeg *et al.*, 2015; Scourse *et al.*, 2019). The advance of the ISIS was larger, extending 550 km to the south Celtic Sea (Praeg *et al.*, 2015; Lockhart *et al.*, 2018; Scourse *et al.*, 2019) and it was also faster, at ~180 m a^{-1}. Comparison of the timing for the LGM in the English Midlands with other global ice-sheets is better framed in the context of the response of the entire BIIS, although the Irish Sea sector was a large ice mass discharging >17% of the total BIIS. The LGM maxima for the Irish Sea sector displays a strong similarity in timing to the other west-draining and marine-terminating ice streams of the former BIIS (Callard *et al.*, 2018; Ó Cofaigh *et al.*, 2019; Scourse *et al.*, 2019; Callard *et al.*, 2020). The LGM in the English Midlands, expanding after 28.3 ± 1.9 ka and reaching the maximum limit at 26.5 ± 1.8 ka, is early in the context of an LGM during GS-3 at 27.5–23.3 ka (Hughes and Gibbard, 2015) and it is early also in the time window for the eustatic sea-level minimum and maximum global ice volume (Fig. 15) (Lambeck *et al.*, 2014). This relatively early build-up and expansion of ice reflects potentially the wetter oceanic climate on the Atlantic eastern seaboard during the prolonged colder conditions of late MIS 3 and GS-5, and was followed by substantial glacier growth during the cold conditions of GS-3 (Rasmussen *et al.*, 2014, 2016).

Retreat of the ISG was initially slow and relatively even in pace, with ice margins passing through the ~80 km of Shropshire and Cheshire between *25.3 ± 1.6* and *22.5 ± 1.0* ka at net rates of ~30 m a^{-1} (Fig. 15A). This retreat begins under cooler conditions of GS-3 and with cold surface waters in the North Atlantic (Fig. 15C,D), posing the question: why is the land-terminating ISG retreating? A possible explanation lies in the ISG sharing the same source regions as the larger ISIS, an ice mass that underwent a ~550-km advance at net advance rates of 180 m a^{-1}. The extension of the ISIS into the Celtic Sea was short-lived (Scourse *et al.*, 1990, 2019; Ó Cofaigh and Evans, 2007; Chiverrell *et al.*, 2013), and was followed by a 500- km retreat coeval with Heinrich Event H2 at net retreat rates of 150 m a^{-1} (Smedley *et al.*, 2017a). These ice margin retreat rates are five times faster than the coeval slower retreat of the ISG from the English Midlands. The discharge of ice to the Celtic Sea effectively beheaded the ISG in the English Midlands, which would account for the ubiquitous evidence for ice stagnation and disintegration topography in the form of kettle-holes throughout the retreat sequence in the English Midlands (Thomas, 1989, 2005; Chiverrell *et al.*, 2016). Net ice-marginal retreat rates then accelerated with the step back of ice margins into the Irish Sea and Lancashire covering ~130 km at ~70 m a^{-1}, before slowing as the ice margins stepped back into the Lake District (Fig. 15A). The increase in pace of retreat around *22.5 ± 1.0 ka* corresponds with a number of factors including

increasing June insolation (Fig. 15A) and higher temperatures during Greenland Interstadial 2 (GI-2: Fig. 15C,D), wider ice margins and increasing influence of calving margin initially in the broader deeper glacial lakes of the lower Dee and Weaver basins and latterly in the glacimarine eastern Irish Sea (Smedley *et al.*, 2017a; Chiverrell *et al.*, 2018). Our interpretation of this retreat sequence highlights the importance of considering the competition between glaciers and internal dynamics in controlling the behaviour of ice-masses during retreat episodes.

The ISG was the dominant ice mass in the English Midlands, but moraines reflecting ice issuing from the Severn and other valley systems evidence a lobate readvance of Welsh ice taking advantage probably of the accommodation space vacated by Irish Sea ice. Welsh ice moraines appear a corollary of equivalent ISG moraines near Wood Lane dated to *23.9 ± 1.0 ka* (Fig. 9) and the outwash deposits of Welsh ice have been dated here for first time at Condover to 19.7 ± 2.5 ka. There are lobate moraines on the sea floor west of Wales, and ice-sheet modelling experiments (Patton *et al.*, 2013) have pointed to a westwards readvance by Welsh Ice after the retreat of the ISIS that is undated but postulated at around 21 ka. There was a readvance by Welsh ice both to the east and to the west after the retreat of Irish Sea ice, and this is constrained here to the period *23.9 ± 1.0* to 19.7 ± 2.5 ka. Hughes *et al.* (2016b) dated the thinning of the Welsh Ice Cap using 15 ^{10}Be ages. Those measurements have been recalculated here using Loch Lomond Production Rates (Fabel *et al.*, 2012) and combined with a reduced Chi-square test ($\chi^2 = 21$; 5% = 23.7) to give an age of 20.7 ± 0.23 ka. A Welsh readvance is more difficult to sustain later during the period *23.9 ± 1.0* to 19.7 ± 2.5 ka with the Welsh Ice Cap thinning by 20.7 ± 0.23 ka. These constraints place the Welsh readvance during the transition to colder conditions from GI-3 to GS-2 (Rasmussen *et al.*, 2014, 2016). The forcing of the readvance could also have included an opportunistic expansion to occupy the accommodation space vacated by the ISG. The lobate Welsh moraines are located on the western shoreline on an over-deepened basin, Glacial Lake Severn (Fig. 7), which raises glacier instability at the transition from land-terminating to a calving glacilacustrine ice margin as a further possible forcing mechanism. This convergence of a cooler climate, accommodation space and dynamic instability owing to ice-bed topography and environments provided conditions conducive to and explaining the readvance and oscillation of the Welsh ice margin in the English Midlands.

Conclusions

We present a novel combination of cobble-, SA- and SG-OSL to constrain the timing of BIIS advance to LGM limits in the English Midlands and the pace of ice margin retreat. New geomorphological mapping and assessment of the glacial stratigraphy at key sites have revealed the evolution of environments fronting the ice margins during deglaciation of the region. Patterns in this geochronology provide the first constraint on what, from a global perspective, is an early build-up and advance of ice into lowland Lancashire during GS-5 at *30 ± 2.0 ka*, with the advance to terrestrial LGM limits during GS-3 between *28.3 ± 1.9 ka* and a maximum extent at *26.5 ± 1.8 ka*. This land-terminating advance slightly pre-dates or is coeval with the large expansion of the ISIS into the south Celtic Sea. Evidence for a reduced ice presence on the ISG eastern ice margins fronting eastern Lake District ice and endemic ice stagnation and disintegration topography accompanied the relatively early retreat of ice from the English Midlands during GS-3. The correspondence of these events point to the ISIS Celtic Sea advance and onset of ice streaming in the central Irish Sea as key internal drivers of the glacial dynamics. The advance of ice to maximum limits occurs during the climate cooling and summer insolation minima of GS-3. Thereafter, still under the cooler conditions of GS-3, piracy of shared ice sources by the ISIS led to a decline in impetus behind the ISG feeding towards the English Midlands. In the English Midlands the ISG retreat was slow and relatively even in pace between *25.3 ± 1.6* and *22.5 ± 1.0* ka. The establishment and abandonment of a series of time transgressive lakes accompanied the retreat of ice margins from the English Midlands. Retreat of ice margins from the larger and deeper of these lakes in the lower River Dee and Weaver basins provides a possible explanation for the acceleration in retreat around *22.5 ± 1.0 ka* with the ice front eventually vacating the region by *20.6 ± 2.2 ka*, but this also corresponds with increasing June insolation and higher temperatures of GI-2. The geomorphology west of Shrewsbury shows unambiguous evidence for what might be an opportunistic readvance of Welsh ice as the Severn Valley Glacier expanded into space vacated by the ISG between *23.9 ± 1* and 19.7 ± 2.5 ka, but this also corresponds with the GI-3 to GS-2 transition to colder conditions and occurred in a location conducive to ice margin instability on the down-ice shoreline of a substantial glacial over-deepening.

In summary, we have shown a GS-5 build-up and then GS-3 expansion of Irish Sea ice into the English Midlands, which reflects potentially wetter oceanic conditions affecting the BIIS on the Atlantic eastern seaboard during these cold episodes. The timescale and geomorphology of the English Midlands retreat sequence point to a glacial system driven by climate, but heavily mediated by competition between ice masses, internal adjustments in the flow regime and the nature of the environment fronting the ice margins during the advance and retreat from maximum limits.

Supporting information

Additional supporting information may be found in the online version of this article at the publisher's web-site.

Acknowledgements. This work was supported by a Natural Environment Research Council consortium grant: BRITICE-CHRONO NE/J009768/1. Thanks are due to the technical support staff at the Aberystwyth Luminescence Research Laboratory and Sheffield Luminescence Laboratory. Phil Hughes, an anonymous reviewer and the editorial input of Arjen Stroeven are acknowledged for their detailed constructive comments, which helped to improve the paper.

Data availability statement

The data that support the findings of this study are available from the corresponding author upon reasonable request.

Abbreviations. BGS, British Geological Survey; BIIS, British–Irish Ice Sheet; GS, Greenland Stadial; ICP-AES, inductively coupled plasma atomic emission spectroscopy; ICP-MS, inductively coupled plasma mass spectrometry; IEU, internal–external uncertainty; IRSL, infra-red stimulated luminescence; ISB, Irish Sea Basin; ISG, Irish Sea Glacier; ISIS, Irish-Sea Ice Stream; LGM, Last Glacial Maximum; MAM, Minimum Age Model; MCMC, Markov chain Monte Carlo; MIS, Marine Isotope Stage; OSL, optically stimulated luminescence; RVG, Ribble Valley Glacier; SA, small aliquots; SG, single grains; SVG, Severn Valley Glacier.

References

Aitkenhead N, Bridge D, Riley NJ *et al.* 1992. *Geology of the Country Around Garstang. Memoir of the British Geological Survey, Sheet 67*. HM Stationery Office: London.

Auclair M, Lamothe M, Huot S. 2003. Measurement of anomalous fading for feldspar IRSL using SAR. *Radiation Measurements* **37**: 487–492.

Bateman MD, Evans DJA, Roberts DH *et al*. 2018. The timing and consequences of the blockage of the Humber Gap by the last British–Irish Ice Sheet. *Boreas* **47**: 41–61.

Berger A, Loutre MF. 1991. Insolation values for the climate of the last 10 million years. *Quaternary Science Reviews* **10**: 297–317.

Bond G, Heinrich H, Broecker W *et al*. 1992. Evidence for massive discharges of icebergs into the North Atlantic Ocean during the last glacial period. *Nature* **360**: 245–249.

Bos JAA, Dickson JH, Coope GR *et al*. 2004. Flora, fauna and climate of Scotland during the Weichselian–Middle Pleniglacial – palynological, macrofossil and coleopteran investigations. *Palaeogeography, Palaeoclimatology, Palaeoecology* **204**: 65–100.

Bøtter-Jensen L, Mejdahl V. 1988. Assessment of beta dose-rate using a GM multicounter system. *International Journal of Radiation Applications and Instrumentation. Part D. Nuclear Tracks and Radiation Measurements* **14**: 187–191.

Bradley SL, Milne GA, Shennan I *et al*. 2011. An improved glacial isostatic adjustment model for the British Isles. *Journal of Quaternary Science* **26**: 541–552.

Brazier V, Kirkbride MP, Gordon JE. 1998. Active ice-sheet deglaciation and ice-dammed lakes in the northern Cairngorm Mountains, Scotland. *Boreas* **27**: 297–310.

Bronk Ramsey C. 2009a. Bayesian analysis of radiocarbon dates. *Radiocarbon* **51**: 337–360.

Bronk Ramsey C. 2009b. Dealing with outliers and offsets in radiocarbon dating. *Radiocarbon* **51**: 1023–1045.

Bronk Ramsey C, Lee S. 2013. Recent and planned developments of the program OxCal. *Radiocarbon* **55**: 720–730.

Bronk Ramsey CB. 2008. Deposition models for chronological records. *Quaternary Science Reviews* **27**: 42–60.

Brown EJ, Rose J, Coope RG *et al*. 2007. An MIS 3 age organic deposit from Balglass Burn, central Scotland: palaeoenvironmental significance and implications for the timing of the onset of the LGM ice sheet in the vicinity of the British Isles. *Journal of Quaternary Science* **22**: 295–308.

Buck CE, Cavanagh WG, Litton CD. 1996. *Bayesian Approach to Interpreting Archaeological Data*. Wiley: Chichester: 1.–402.

Callard SL, Cofaigh CÓ, Benetti S *et al*. 2018. Extent and retreat history of the Barra Fan Ice Stream offshore western Scotland and northern Ireland during the last glaciation. *Quaternary Science Reviews* **201**: 280–302.

Callard SL, Ó Cofaigh C, Benetti S *et al*. 2020. Oscillating retreat of the last British–Irish Ice Sheet on the continental shelf offshore Galway Bay, western Ireland. *Marine Geology* **420**.

Cannell B. 1982. *The Sand and Gravel Resources of the Country Around Shrewsbury, Shropshire: Description of 1: 25000 Sheets SJ41 and SJ51*. London: Institute of Geological Sciences.

Cannell B, Harries WRJ. 1981. *The Sand and Gravel Resources of the Country Around Wem, Shropshire: Description of 1: 25 000 Sheets SJ42 and SJ52*. London: Institute of Geological Sciences.

Chiverrell RC, Burke MJ, Thomas GSP. 2016. Morphological and sedimentary responses to ice mass interaction during the last deglaciation. *Journal of Quaternary Science* **31**: 265–280.

Chiverrell RC, Smedley RK, Small D *et al*. 2018. Ice margin oscillations during deglaciation of the northern Irish Sea Basin. *Journal of Quaternary Science* **33**: 739–762.

Chiverrell RC, Thomas GSP. 2010. Extent and timing of the Last Glacial Maximum (LGM) in Britain and Ireland: a review. *Journal of Quaternary Science* **25**: 535–549.

Chiverrell RC, Thomas GSP, Foster GC. 2008. Sediment–landform assemblages and digital elevation data: testing an improved methodology for the assessment of sand and gravel aggregate resources in north-western Britain. *Engineering Geology* **99**: 40–50.

Chiverrell RC, Thrasher IM, Thomas GSP *et al*. 2013. Bayesian modelling the retreat of the Irish Sea Ice Stream. *Journal of Quaternary Science* **28**: 200–209.

Clark CD, Hughes ALC, Greenwood SL *et al*. 2012. Pattern and timing of retreat of the last British–Irish Ice Sheet. *Quaternary Science Reviews* **44**: 112–146.

Clark PU, Dyke AS, Shakun JD *et al*. 2009. The Last Glacial Maximum. *Science* **325**: 710–714.

Colarossi D, Duller GAT, Roberts HM *et al*. 2015. Comparison of paired quartz OSL and feldspar post-IR IRSL dose distributions in poorly bleached fluvial sediments from South Africa. *Quaternary Geochronology* **30**: 233–238.

De Rance CE 1877. *The Geology of the Country Around Blackpool, Poulton and Fleetwood. Memoir of the Geological Survey of Great Britain: London*.

Dietze M, Kreutzer S, Burow C *et al*. 2016. The abanico plot: visualising chronometric data with individual standard errors. *Quaternary Geochronology* **31**: 12–18.

Duller GAT. 2008. Single-grain optical dating of Quaternary sediments: why aliquot size matters in luminescence dating. *Boreas* **37**: 589–612.

Earp JR, Poole EG, Whiteman AJ 1961. *Geology of the Country Around Clitheroe and Nelson. Memoir of the Geological Survey of Great Britain, 68*. HM Stationery Office: London.

Evans DJA 2003. *Glacial Landsystems*. Arnold: London.

Evans DJA, Bateman MD, Roberts DH *et al*. 2017. Glacial Lake Pickering: stratigraphy and chronology of a proglacial lake dammed by the North Sea Lobe of the British–Irish Ice Sheet. *Journal of Quaternary Science* **32**: 295–310.

Evans DJA, Benn DI 2004. *A Practical* Guide to the Study of Glacial Sediments. Arnold, London. 266pp. ISBN:10: 0340759593.

Fabel D, Ballantyne CK, Xu S. 2012. Trimlines, blockfields, mountain-top erratics and the vertical dimensions of the last British–Irish Ice Sheet in NW Scotland. *Quaternary Science Reviews* **55**: 91–102.

Freiesleben T, Sohbati R, Murray A *et al*. 2015. Mathematical model quantifies multiple daylight exposure and burial events for rock surfaces using luminescence dating. *Radiation Measurements* **81**: 16–22.

Galbraith RF, Laslett GM. 1993. Statistical models for mixed fission track ages. *Nuclear Tracks and Radiation Measurements* **21**: 459–470.

Galbraith RF, Roberts RG, Laslett GM *et al*. 1999. Optical dating of single and multiple grains of quartz from Jinmium rock shelter, northern Australia: Part I, experimental design and statistical models. *Archaeometry* **41**: 339–364.

Gresswell RK. 1967. The geomorphology of Fylde. In *Liverpool Essays in*. In *Geography: a Jubilee Collection*, Stell RW, Lawton R (eds). Longmans: London; 25–42.

Guérin G, Mercier N, Adamiec G. 2011. *Dose-rate conversion factors: update. Ancient TL* **29**: 5–8.

Guérin G, Mercier N, Nathan R *et al*. 2012. On the use of the infinite matrix assumption and associated concepts: A critical review. *Radiation Measurements* **47**: 778–785.

Haapaniemi AI, Scourse JD, Peck VL *et al*. 2010. Source, timing, frequency and flux of ice-rafted detritus to the northeast Atlantic margin, 30–12 ka: testing the Heinrich precursor hypothesis. *Boreas* **39**: 576–591.

Hamblin RJO. 1986. The Pleistocene sequence of the Telford district. *Proceedings of the Geologists' Association* **97**: 365–377.

Harmer FW. 1907. On the origin of certain cañon-like valleys associated with lake-like areas of depression. *Quarterly Journal of the Geological Society* **63**: 470–514.

Hughes ALC, Gyllencreutz R, Lohne ØS *et al*. 2016a. The last Eurasian ice sheets – a chronological database and time-slice reconstruction, DATED-1. *Boreas* **45**: 1–45.

Hughes PD, Gibbard PL. 2015. A stratigraphical basis for the Last Glacial Maximum (LGM). *Quaternary International* **383**: 174–185.

Hughes PD, Gibbard PL, Ehlers J. 2013. Timing of glaciation during the last glacial cycle: evaluating the concept of a global 'Last Glacial Maximum' (LGM). *Earth-Science Reviews* **125**: 171–198.

Hughes PD, Glasser NF, Fink D. 2016b. Rapid thinning of the Welsh Ice Cap at 20–19ka based on ^{10}Be ages. *Quaternary Research* **85**: 107–117.

Huntley DJ, Baril M. 1997. The K content of the K-feldspars being measured in optical dating or in thermoluminescence dating. *Ancient TL* **15**: 11–13.

Huntley DJ, Lamothe M. 2001. Ubiquity of anomalous fading in K-feldspars and the measurement and correction for it in optical dating. *Canadian Journal of Earth Sciences* **38**: 1093–1106.

Jardine WG, Dickson JH, Haughton PDW *et al*. 1988. A late Middle Devensian interstadial site at Sourlie, near Irvine, Strathclyde. *Scottish Journal of Geology* **24**: 288–295.

Jenkins GTH, Duller GAT, Roberts HM *et al*. 2018. A new approach for luminescence dating glaciofluvial deposits – High precision optical dating of cobbles. *Quaternary Science Reviews* **192**: 263–273.

Johnson RH. 1971. The last glaciation in north west England: a general survey. *Amateur Geologist* **5**: 18–37.

King O, Dehecq A, Quincey D *et al*. 2018. Contrasting geometric and dynamic evolution of lake and land-terminating glaciers in the central Himalaya. *Global and Planetary Change* **167**: 46–60.

Kirkbride MP. 1993. The temporal significance of transitions from melting to calving termini at glaciers in the central Southern Alps of New Zealand. *The Holocene* **3**: 232–240.

Kirkbride MP. 1995. Relationships between temperature and ablation on the Tasman Glacier, Mount Cook National Park, New Zealand. *New Zealand Journal of Geology and Geophysics* **38**: 17–27.

Lambeck K, Purcell AP. 2001. Sea-level change in the Irish Sea since the Last Glacial Maximum: constraints from isostatic modelling. *Journal of Quaternary Science* **16**: 497–506.

Lambeck K, Rouby H, Purcell A *et al*. 2014. Sea level and global ice volumes from the Last Glacial Maximum to the Holocene. *Proceedings of the National Academy of Sciences of the United States of America* **111**: 15296–15303.

Livingstone SJ, Evans DJA, Cofaigh C. Ó. 2010. Re-advance of Scottish ice into the Solway Lowlands (Cumbria, UK) during the Main Late Devensian deglaciation. *Quaternary Science Reviews* **29**: 2544–2570.

Livingstone SJ, Evans DJA, Ó Cofaigh C *et al*. 2012. Glaciodynamics of the central sector of the last British–Irish Ice Sheet in Northern England. *Earth-Science Reviews* **111**: 25–55.

Lockhart EA, Scourse JD, Praeg D *et al*. 2018. A stratigraphic investigation of the Celtic Sea megaridges based on seismic and core data from the Irish-UK sectors. *Quaternary Science Reviews* **198**: 156–170.

Longworth D. 1985. The Quaternary history of the Lancashire Plain. In *The Geomorphology of Northwest England*, Johnson RH (ed). Manchester University Press: Manchester; 178–200.

Maw G. 1864. Notes on the drift-deposits of the valley of the Severn, in the Neighbourhood of Coalbrook Dale and Bridgnorth. *Quarterly Journal of the Geological Society* **20**: 130–144.

McCabe AM. 2008. *Glacial Geology and Geomorphology: the Landscapes of Ireland*. Dunedin Academic Press: Edinburgh.

McCabe M, Knight J, McCarron S. 1998. Evidence for Heinrich event 1 in the British Isles. *Journal of Quaternary Science* **13**: 549–568.

Miall AD. 1977. A review of the braided-river depositional environment. *Earth-Science Reviews* **13**: 1–62.

Mitchell WA. 1991. *Western Pennines: a Field Guide*. Quaternary Research Association: London.

Mitchell WA, Hughes ALC. 2012. The Late Devensian glaciation in the Yorkshire Dales. In *Cave Archaeology and Karst Geomorphology of North West England*. In *Quaternary Research Association: London*, O'Regan HJ, Faulkner T, Smith IR (eds)., 34–45.

Morgan AV. 1973. The Pleistocene geology of the area North and west of Wolverhampton, Staffordshire, England. *Philosophical Transactions of the Royal Society of London* **265**: 233–297.

Moros M, Kuijpers A, Snowball I *et al*. 2002. Were glacial iceberg surges in the North Atlantic triggered by climatic warming? *Marine Geology* **192**: 393–417.

Murray AS, Wintle AG. 2000. Luminescence dating of quartz using an improved single-aliquot regenerative-dose protocol. *Radiation Measurements* **32**: 57–73.

Murton DK, Murton JB. 2012. Middle and Late Pleistocene glacial lakes of lowland Britain and the southern North Sea Basin. *Quaternary International* **260**: 115–142.

Nemec W. 2009. Aspects of Sediment Movement on Steep Delta Slopes. *Coarse-Grained Deltas* 29–73.

Nemec W, Lønne I, Blikra LH. 1999. The Kregnes moraine in Gauldalen, west-central Norway: anatomy of a Younger Dryas proglacial delta in a palaeofjord basin. *Boreas* **28**: 454–476.

Ó Cofaigh C, Evans DJA. 2007. Radiocarbon constraints on the age of the maximum advance of the British–Irish Ice Sheet in the Celtic Sea. *Quaternary Science Reviews* **26**: 1197–1203.

Ó Cofaigh C, Weilbach K, Lloyd JM *et al*. 2019. Early deglaciation of the British–Irish Ice Sheet on the Atlantic shelf northwest of Ireland driven by glacioisostatic depression and high relative sea level. *Quaternary Science Reviews* **208**: 76–96.

Ou XJ, Roberts HM, Duller GAT *et al*. 2018. Attenuation of light in different rock types and implications for rock surface luminescence dating. *Radiation Measurements* **120**: 305–311.

Palacios D, Stokes CR, Phillips FM *et al*. 2020. The deglaciation of the Americas during the Last Glacial Termination. *Earth-Science Reviews* 203.

Parkes AA, Waller RI, Knight PG *et al*. 2009. A morphological, sedimentological and geophysical investigation of the Woore Moraine, Shropshire, England. *Proceedings of the Geologists' Association* **120**: 233–244.

Patton H, Hubbard A, Bradwell T *et al*. 2013. Rapid marine deglaciation: asynchronous retreat dynamics between the Irish Sea Ice Stream and terrestrial outlet glaciers. *Earth Surface Dynamics* **1**: 53–65.

Peake DS. 1961. Glacial changes in the Alyn river system and their significance in the glaciology of the North Welsh border. *Quarterly Journal of the Geological Society* **117**: 335–363.

Peake DS. 1979. The limit of the Devensian Irish Sea ice sheet on the north Welsh border. *Quaternary Newsletter* **27**: 1–4.

Peake DS. 1981. The Devensian glaciation on the North Welsh border. *In The Quaternary in Britain* 49–59.

Peck VL, Hall IR, Zahn R *et al*. 2006. High resolution evidence for linkages between NW European ice sheet instability and Atlantic Meridional Overturning Circulation. *Earth and Planetary Science Letters* **243**: 476–488.

Peck VL, Hall IR, Zahn R *et al*. 2007. The relationship of Heinrich events and their European precursors over the past 60 ka BP: a multi-proxy ice-rafted debris provenance study in the North East Atlantic. *Quaternary Science Reviews* **26**: 862–875.

Pocock RW, Wray DA 1925 The Geology of the Country Around Wem. Geological Survey, Memoirs.

Poole EG. 1966. *Geology of the Country Around Nantwich and Whitchurch: (Explanation of One-Inch Geological sheet 122)*. Her Majesty's Stationery Office: London.

Poole EG, Whiteman AJ. 1961. The glacial drifts of the southern part of the Shropshire–Cheshire basin. *Quarterly Journal of the Geological Society* **117**: 91–130.

Praeg D, McCarron S, Dove D *et al*. 2015. Ice sheet extension to the Celtic Sea shelf edge at the Last Glacial Maximum. *Quaternary Science Reviews* **111**: 107–112.

Price D 1963. *Geology of the Country Around Preston, 75*. H M Stationery Office: London.

Rasmussen SO, Bigler M, Blockley SP *et al*. 2014. A stratigraphic framework for abrupt climatic changes during the Last Glacial period based on three synchronized Greenland ice-core records: refining and extending the INTIMATE event stratigraphy. *Quaternary Science Reviews* **106**: 14–28.

Rasmussen TL, Thomsen E, Moros M. 2016. North Atlantic warming during Dansgaard-Oeschger events synchronous with Antarctic warming and out-of-phase with Greenland climate. *Scientific Reports* **6** 20535.

Sambrook Smith GH, Ashworth PJ, Best JL *et al*. 2005. The morphology and facies of sandy braided rivers: some considerations of scale invariance. *Special Publications of the International Association of Sedimentologists* **35**: 145–158.

Sambrook Smith GH, Ashworth PJ, Best JL *et al*. 2006. The sedimentology and alluvial architecture of the sandy braided South Saskatchewan River, Canada. *Sedimentology* **53**: 413–434.

Scourse JD, Austin WEN, Bateman RM *et al*. 1990. Sedimentology and micropalaeontology of glacimarine sediments from the Central and southwestern Celtic Sea. In *Glacimarine Environments: Processes and Sediments*, Dowdeswell JA, Scourse JD (eds). Special Publication of the Geological Society. The Geological Society of London: London.

Scourse JD, Coope GR, Allen JRM *et al*. 2009. Late-glacial remains of woolly mammoth (*Mammuthus primigenius*) from Shropshire, UK: stratigraphy, sedimentology and geochronology of the Condover site. *Geological Journal* **44**: 392–413.

Scourse J, Saher M, Van Landeghem KJJ *et al*. 2019. Advance and retreat of the marine-terminating Irish Sea Ice Stream into the Celtic Sea during the last glacial: timing and maximum extent. *Marine Geology* **412**: 53–68.

Shaw J. 1972a. The Irish Sea glaciation of north Shropshire – some environmental reconstructions. *Field Studies* **4**: 603–631.
Shaw J. 1972b. Sedimentation in the ice-contact environment with examples from Shropshire (England). *Sedimentology* **18**: 23–62.
Small D, Smedley RK, Chiverrell RC *et al*. 2018. Trough geometry was a greater influence than climate-ocean forcing in regulating retreat of the marine-based Irish-Sea Ice Stream. *GSA Bulletin* **130**: 1981–1999.
Smedley RK, Chiverrell RC, Ballantyne CK *et al*. 2017a. Internal dynamics condition centennial-scale oscillations in marine-based ice-stream retreat. *Geology* **45**: 787–790.
Smedley RK, Duller GAT, Rufer D *et al*. 2020. Empirical assessment of beta dose heterogeneity in sediments: implications for luminescence dating. *Quaternary Geochronology* 56.
Smedley RK, Scourse JD, Small D *et al*. 2017b. New age constraints for the limit of the British–Irish Ice Sheet on the Isles of Scilly. *Journal of Quaternary Science* **32**: 48–62.
Smith ND, Ashley GM. 1985. Proglacial lacustrine environment. *In Glacial Sedimentary Environments* 135–216.
Sohbati R, Murray AS, Porat N *et al*. 2015. Age of a prehistoric 'Rodedian' cult site constrained by sediment and rock surface luminescence dating techniques. *Quaternary Geochronology* **30**: 90–99.
Stokes CR. 2018. Geomorphology under ice streams: moving from form to process. *Earth Surface Processes and Landforms* **43**: 85–123.
Stokes CR, Clark CD. 1999. Geomorphological criteria for identifying Pleistocene ice streams. *Annals of Glaciology* **28**: 67–74.
Telfer MW, Wilson P, Lord TC *et al*. 2009. New constraints on the age of the last ice sheet glaciation in NW England using optically stimulated luminescence dating. *Journal of Quaternary Science* **24**: 906–915.
Thiel C, Buylaert JP, Murray A *et al*. 2011. Luminescence dating of the Stratzing loess profile (Austria) – Testing the potential of an elevated temperature post-IR IRSL protocol. *Quaternary International* **234**: 23–31.
Thomas GSP. 1985a. The Late Devensian glaciation along the border of northeast Wales. *Geological Journal* **20**: 319–340.
Thomas GSP 1985b. The Quaternary of the Northern Irish Sea Basin. In *The Ggeomorphology of North-West England*, Johnson RH (ed). Manchester University Press: Manchester; 143–158.
Thomas GSP. 1989. The Late Devensian glaciation along the western margin of the Cheshire–Shropshire lowland. *Journal of Quaternary Science* **4**: 167–181.
Thomas GSP. 2005. North-East Wales. In *The Glaciations of Wales and Adjacent Areas*, Lewis CA, Richards AE (eds). Logaston Press: Bristol; 41–58.
Thomas GSP, Chiverrell R, Huddart D. 2004. Ice-marginal depositional responses to readvance episodes in the Late Devensian deglaciation of the Isle of Man. *Quaternary Science Reviews* **23**: 85–106.
Thomas GSP, Chiverrell RC. 2007. Structural and depositional evidence for repeated ice-marginal oscillation along the eastern margin of the Late Devensian Irish Sea Ice Stream. *Quaternary Science Reviews* **26**: 2375–2405.
Thomas GSP, Connaughton M, Dackombe RV. 1985. Facies variation in a Late Pleistocene supraglacial outwash sandur from the Isle of Man. *Geological Journal* **20**: 193–213.
Thomsen KJ, Murray AS, Bøtter-Jensen L *et al*. 2007. Determination of burial dose in incompletely bleached fluvial samples using single grains of quartz. *Radiation Measurements* **42**: 370–379.
Van Kreveld S, Sarnthein M, Erlenkeuser H *et al*. 2000. Potential links between surging ice sheets, circulation changes, and the Dansgaard-Oeschger Cycles in the Irminger Sea, 60-18 Kyr. *Paleoceanography* **15**: 425–442.
Van Landeghem KJJ, Wheeler AJ, Mitchell NC. 2009. Seafloor evidence for palaeo-ice streaming and calving of the grounded Irish Sea Ice Stream: implications for the interpretation of its final deglaciation phase. *Boreas* **38**: 111–118.
Waelbroeck C, Lougheed BC, Vazquez Riveiros N *et al*. 2019. Consistently dated Atlantic sediment cores over the last 40 thousand years. *Scientific Data* **6**: 165.
Watts WW. 1898. Long Excursion to the Birmingham District. *Proceedings of the Geologists' Association* **15**: 417–IN1.
Wedd CB, Smith B, Wills LJ *et al*. 1927. *The Geology of the Country Around Wrexham: Explanation of One-Inch Geological sheet 121, New Series. Memoirs of the Geological Survey of Great Britain, England and Wales (Sheet – New Series)*. HMSO: London.
Whitehead TH, Robertson T, Pocock RW *et al*. 1928. *The Country Between Wolverhampton and Oakengates*. HMSO: London.
Wills LJ. 1948. *The Palaeogeography of the Midlands*. University Press of Liverpool: Liverpool.
Wills LJ, Dixon EEL. 1924. The development of the Severn valley in the neighbourhood of Iron-Bridge and Bridgnorth. *Quarterly Journal of the Geological Society* **80**: 274–308.
Wilson AC, Mathers SJ, Cannell B 1982. The Middle Sands, a prograding sandur succession; its significance in the glacial evolution of the Wrexham- Shrewsbury region. United Kingdom, Institute of Geological Sciences Report 82: 30–35.
Wilson P, Barrows TT, Lord TC 2012a. Cosmogenic isotope analysis and surface exposure dating in the Yorkshire Dales. In *Cave Archaeology and Karst Geomorphology of North West England*, Regan HJO, Faulkner T, Smith IR (eds). Quaternary Research Association and British Cave Research Association: London; 117–135, ISBN: 090778084925323.
Wilson P, Barrows TT, Lord TC *et al*. 2012b. Surface lowering of limestone pavement as determined by cosmogenic (^{36}Cl) analysis. *Earth Surface Processes and Landforms* **37**: 1518–1526.
Wilson P, Lord T. 2014. Towards a robust deglacial chronology for the northwest England sector of the last British–Irish Ice Sheet. *North West Geography* **14**: 1–11.
Wilson P, Lord T, Rodés Á. 2013. Deglaciation of the eastern Cumbria glaciokarst, northwest England, as determined by cosmogenic nuclide (^{10}Be) surface exposure dating, and the pattern and significance of subsequent environmental changes. *Cave and Karst Science* **40**: 22–27.
Wilson P, Rodés Á, Smith A. 2018. Valley glaciers persisted in the Lake District, north-west England, until ~16–15 ka as revealed by terrestrial cosmogenic nuclide (10Be) dating: a response to Heinrich event 1? *Journal of Quaternary Science* **33**: 518–526.
Worsley P 1975. An appraisal of the glacial Lake Lapworth concept. In *Environment, Man and Economic Change*, Phillips ADM, Turton BJ (eds). Longman: London; 98–118.
Worsley P 1985. Pleistocene history of the Cheshire–Shropshire Plain. In *The Geomorphology of North-West England*, Johnson RH (ed). Manchester University Press: Manchester; 201–221.
Worsley P. 2005. The Cheshire–Shropshire plain. In *The Glaciations of Wales and Adjacent Areas*, Lewis CA, Richards AE (eds). Logaston Press: Bristol; 59–72.

